

Magneto-thermal instabilities in type II superconductors

N.A. Taylanov

National University of Uzbekistan

Abstract

Magneto-thermal instabilities are one of the peculiar phenomena of interest in conventional type-II, as well as in high- T_c superconductors. In the present paper we attempt to analyze the nature and origin of the magneto-thermal instabilities of the critical state and flux jumps phenomena in superconductors in the light of recent theoretical and experimental results.

Key words: critical state, flux jumps, flux avalanches, flux flow and flux creep, second magnetization peak, instability

Introduction

The magnetic flux penetration into a type-II superconductor occurs in the form of quantized vortices. Each of these vortices has a normal core, which presents a long cylinder with a radius comparable to the superconducting coherence length ξ . Undamping superconducting current flows around this cylinder. The vortex current seizes an area of radius of order of penetration depth λ . Each vortex carries one magnetic flux quantum, which determined by the equality $\phi_0 = 2 \div 10^7 \text{ Gs} \cdot \text{sm}^2$. The penetration of the vortex into the superconductor becomes energetically favorable at the field H_{c1} . The vortices are located one after another on the distance λ forming correct triangular lattice in the superconductor at the interval $H_{c1} \ll H \ll H_{c2}$; where H_{c1} and H_{c2} are the lower and upper critical magnetic fields. With increasing magnetic field the period of lattices decreases and the vortex density increases. At the field H_{c2} the vortex density becomes so great that the period of lattices becomes an order of coherence length ξ . This means that magnetic flux completely penetrates into the superconductor and second type phase transition to the normal state occurs. In the interval of fields $H_{c1} \ll H \ll H_{c2}$ superconductor is in the mixed state. In the presence of different types of defects or pinning centers in the superconductor sample, the vortices may be attached to such defects. A nature of interaction between the vortices and the structural defects is determined by the pinning force F_P . If transport current with the density j is passed through superconductor, the interaction of the current with vortex lines leads to the emergence of the Lorentz force F_L , acting on each one of the vortices. Under the effect of the Lorentz force F_L the viscous flux flow of vortices begin to move. The viscous magnetic flux flow in accordance with electromagnetic induction creates a vortex electric field E . This means that energy dissipation occurs, an electric resistance appears and the superconductor undergoes a transition to the resistive or to the normal state. Propagating magnetic flux causes Joule heating, giving rise to global and/or micro flux avalanches in the critical state of type-II superconductors. Thus flux jumps results in a large-scale flux avalanches in a superconductor and their origin are related to the magneto-thermal instabilities.

Magneto-thermal instabilities of the critical state and flux jump phenomenon in hard superconductors with high values of the critical current density and the critical magnetic fields have been investigated since 1960's in a classical works of Bean and et al. [1-3]. A detailed qualitative analysis of the magnetic in-

stabilities in type-II superconductors was given by Wipf [4]. The magnetic flux jumps were studied in Refs. [5, 6] for a linear voltage-current characteristics of superconductor in the framework of adiabatic approximation i.e., assuming that the thermal diffusion, is much smaller than the magnetic flux diffusion. The criterion for the stability of the critical state in the case of dynamic approximation was obtained by Kremlev [7]. The general concept of the magnetic instabilities in type-II superconductors was developed in literature [8]. The thermal and electromagnetic processes, whose development leads to the flux jump, have been investigated in detail and the stability criterion have been found in the framework of adiabatic and dynamic approximations in the viscous flux flow regime by Mints and Rakhmanov [9]. The detailed theoretical analyze of the flux jumping in the flux creep regime where the current-voltage characteristics of type-II superconductors is a nonlinear have been carried out recently by Mints [10] and by Mints and Brandt [11].

The dynamics of magneto-thermal instabilities has been recently extensively studied in hard type-II as well as high T_c superconductors. And several contrasting models have been proposed for the detailed description for the nature of their origin and dynamics. The dynamics and the nature of observed in recent magnetization measurements of various techniques flux jumps can be explained in the scenario of magneto-thermal instability theory [1]. According to this theory moving flux lines increase the local temperature T and therefore reduce the critical current density j_c , which triggers further flux motion. This positive feedback may result in a magnetic flux avalanches and thermal instabilities in the superconductor sample. It is notice able that a recent theoretical and experimental investigations show that the dynamics of these flux jump instabilities strongly depends on the local temperature change, the rate of field change, the critical current density and its temperature and field derivatives, the ratio between thermal conductivity and heat capacity, the sample geometry, cooling conditions, pinning and micro-structural properties of a considered superconducting material.

Many experimental and theoretical investigations on magneto-thermal instabilities in low and high- T_c superconducting materials with different shapes and geometries, including thin Nb, MgB_2 films, organic superconductors and layered compounds, single and textured crystals, rings and bulk samples have been recently reported. However, no systematic studies of this problem have been reported and there is little understanding as to how different internal and external parameters affect flux

arXiv:1111.1416v1 [cond-mat.supr-con] 6 Nov 2011

jumping behaviors in a various superconducting samples.

Interestingly that most magnetization measurements show that the flux jumps occur at lower magnitudes of temperature and magnetic fields in a single superconductor material. Some experimental results show that flux jumps occur at temperatures and magnetic fields larger than the full penetration field H_p , but lower than the H_{c1} . For instance, magnetothermal instabilities in organic type-II superconductors have been observed in the form of abrupt flux jumps at extremely low temperatures by Mola et al. [12] by means a torque magnetometer. Based on analysis of the temperature dependence of the jumps they found that the amplitude of the observed flux jumps increases with temperature as $A \sim T^{3/2}$, which consistent with accepted models. They have showed that as the temperature is increased the flux jumps are observed less frequently, and with greater magnitude. Thus, the authors believed that the sudden cessation of the flux jumps above a characteristic field B_j , which decreases upon increasing the temperature. It was also found that the average amplitude of the flux jumps is an increasing function of angle having an $A(\Theta) \approx 1 - \cosh(\Theta)$ dependence.

Similar temperature and field dependencies of the flux jump instabilities have been observed by Radovan and Zieve [13] in their local Hall probe measurements. They found both large and small flux jumps at different temperatures in a type-II thin Pb film superconductors. The flux jumps occur only at very low applied fields. A large jumps observed only at relatively high temperatures. It has been shown by these authors that at sufficiently low temperatures the jump size decreases roughly as T^3 , approaching a finite value at zero temperature. They found a power law distributions of avalanche size at temperatures $T = 0.3$ K and $T = 4.3$ K with corresponding exponents of 2.01 and 1.09, respectively. Thus the authors argued that an interplay between vortex density and the microstructure is at the origin of the flux instabilities.

The strong temperature dependence of the magnitude and frequency of flux jumps have been observed by Nowak and his co-workers [14] in a ring-shaped Nb thin films using a Hall probes. The magnetization of the film was measured at $T = 1.4 \div 10$ K as a function of temperature and applied field, perpendicular to the plane of the sample. At $T \sim 3.1$ K has been detected a crossover from a broad to narrow of the size distribution of internal avalanches in the rings. The authors argued that the small value of specific heat at low temperatures is at the origin of these jumps in magnetization curves. So, these low-temperature huge avalanches in the rings may be qualitatively understood in a thermal instability scenario [9], according which at low temperatures the vortex motion can result in a local temperature rise. The temperature rise leads to a decrease in the critical current density and therefore magnetothermal instability is produced. The stability parameter β [8, 9] numerically has been calculated by using the measured temperature dependencies of the critical current density j_c and heat capacity $\nu \sim T^3$. The authors found that at highest temperatures thermal effects are negligible and a largest in magnitude heat capacity serves as a stabilizing factor of the Bean's critical state.

A such type of flux jumps in the magnetization curves at low temperatures for a single YBaCuO crystals with a different transition temperatures T_c has been found by Khene and Barbara [15]. It was shown that the first flux jump field B_j depends not only on critical current density j_c and specific heat ν , but also

on the field sweep rate and the transition temperature T_c of the sample. The results of their magnetization measurements show that the field for the first flux jump B_j increases as temperature increases and the flux jumps disappear at higher temperatures. The results obtained in this work suggest a better thermal and magnetic stability for considered single crystals with low transition temperature T_c . The effect of magnetic field sweep rate on the behavior of flux jumps has also been investigated. The field B_j decreases with increasing magnetic field sweep rate \dot{B}_c . Interestingly that these results are very similar to those obtained in conventional II-type superconductors [16].

A more detailed the temperature and magnetic field sweep rate dependencies of flux jumping has been analyzed by Nabialek et al. [17] at temperature of 4.2 K in polycrystalline single crystals by means of magnetization, screening and torque measurements. It has been shown that as the sweep rate decreases the value of the first flux jump field B_j increases rapidly and tends to saturate at higher sweep rates. Similar strong sweep rate dependence on the first flux jump field B_j early has been observed in other experiments of McHenry [18] and Guillot [19]. Nabialek et al. [17], also investigated the temperature dependence of flux jumping, as well as the influence of flux creep and demagnetizing effects on the critical state stability.

The behavior of flux jumps with different amplitudes in superconductors have studied Vanacken et al. [20] using pulsed field magnetization measurements. The time dependence of the flux jumps was presented. A periodical jumps were observed for both the positive and negative field polarities. Surprisingly that the sharp flux jumps occur at lowering magnitude of the field for all temperatures below $T = 30$ K. These jumps are expected to be equidistant $B_j \approx 0.3$ T. As has been shown that the flux jumps strongly depend on the magnetic field sweep rate and the magneto-thermal history of the sample, on the temperature and the critical current density. Such dependence of occurrence of flux jump field on the sweep rate of external magnetic field and the temperature for the melt-textured superconductor materials has been studied by Fuchs et al. [21] at temperatures $T > 20$ K. The observed magnetic instabilities were discussed within the framework of existing theoretical results.

Recently Zhao et al. [22] have observed many multiple small and irregular flux jump instabilities in MgB_2 thin films at temperature below 2 K and applied field of 1.3 T by means a SQUID magnetometer measurements. The magnitude of these instabilities are much larger in low fields than in high fields. With increasing of temperature the small instabilities evolved into some larger ones and disappear completely at temperature $T = 14$ K. The authors believed that there are many places for the avalanche to occur due to a high density of small defects formed during the preparation process of the thin films leading to much stronger critical current densities. As pointed authors thermal diffusion is much easier in thin films due to their very small thickness and large surface area exposed to the environment and consequently, in thin films each avalanche is small in magnitude but the number of avalanches can be huge. The authors argued that this simple picture may give an explanation to many small flux jumps observed in superconducting thin films. They reported the observation of the suppression of the critical current density at low temperatures due to many small jumps in thin films.

Muller and Andrikidis [23] using a SQUID magnetometer has measured the magnetization loop for a melt-textured high T_c su-

perconductors at different temperature and magnetic field intervals. The first flux jump occur at temperature $T=3.0$ K in the magnetization loop, when the applied field is perpendicular to the crystallographic c axis of the sample. At temperature $T=3.5$ K solitary jumps were found and above 3.9 K no flux jumps occur in the magnetization curve. With increasing temperature the first jump field increases and at higher temperatures (above $T=3.05$ K) flux jump suddenly disappears. The measured values of B_j has been compared with existing theoretical results [8, 9]. In this work the stability criterion for flux jumps has been analytically calculated using Kim-Anderson critical state model.

Chabanenko et al. [24] have studied magnetothermal instabilities and giant flux jumps, both theoretically and experimentally in the framework of adiabatic approximation using various dependencies of the critical current density on the magnetic field. In particular, they have numerically calculated magnetization and magnetostriction loops with flux jumps employing the Kim-Anderson critical state model and exponential model for the dependence $j_c(H)$. On the basis of these theoretical calculations it has been constructed a H-T phase diagram of flux jump instabilities. The authors showed that the maximum value of temperature after the flux jump strongly depends on the magnetic field sweep rate and micro-structural properties of the sample.

Vasilev et al. [25] experimentally studied the time of duration of the flux jumps and amount of the magnetic flux entering into a disc type of superconductor sample as a function of temperature and external magnetic field. In another paper Chabanenko et al. [26] have studied the structure of the flux jumps in different superconducting samples, such as Nb-Ti samples, polycrystalline Nb plates and melt-textured YBaCuO slabs on the basis of a temporal dependence of the surface magnetic induction using a miniature Hall probe sensors. The authors have observed very interesting oscillating phenomena originated by the thermomagnetic avalanches in the vortex matter for both low and high- T_c superconductor samples. These oscillation can be qualitatively interpreted in terms of the theoretical model which takes into account the existence of a definite value of the effective vortex mass, i.e the inertial properties of the vortex system [27]. In this work a details of three stages of the thermomagnetic instability development was also proposed.

The influence of the time-dependent external conditions on the stability threshold of the critical state for hard type-II superconductors has been studied theoretically by Mints and Rakhmanov [28]. They found a stability criterion of the critical state as a function of the rate of variation of the external magnetic field and the external temperature in hard superconductors. The authors argued that the existence of a background electric field induced by a variable external magnetic field is essential for observing a temperature and electric field oscillations in a superconductor sample. Similar magnetothermal oscillations in the form of flux jumps have been observed by Kumm et al. [29] in a melt-textured crystals in external varying magnetic field. The interval ΔB_e between consecutive jumps increases with sweep rate \dot{B}_e and decreases with temperature. Every jump is preceded by oscillations of the induced voltage and the sample temperature. A similar oscillations preceding the flux jump instabilities have been studied by numerous researchers in earlier both experimentally by Shimamoto [30] and theoretically by Maksimov and Mints [31]. Earlier Zebouni et al. [32] have detected that the period of oscillations increases strongly with increasing tem-

perature. The oscillations disappear sharply if the sweep was stopped. This effect due to the simultaneous and sharp drop of the sample temperature to the bath temperature. Such a series of heating pulses of very large amplitude appeared at discrete reproducible values of B . The pulses were observed in decreasing field, but at relatively lower values of B . Simultaneously with each of these heat pulses, sudden penetration of magnetic flux was observed. Therefore the pulses related to discontinuous steps in the magnetic flux penetration - flux jumps. A tentative identification of these fluctuations with one of the collective modes of vibration of the vortices predicted by de Gennes and Martison [33]. Such limited flux jump instabilities, initiated by a varying external magnetic field perturbation has been observed in ceramic high- T_c superconductors by Bodi et al. [34]. An extensive study of the magnetothermal oscillations and limited flux jumps in a high- T_c superconductor samples was given by Legrand et al. [35]. Later Legrand et al. [36] have proposed that the magneto-thermal oscillations in the Bean's critical state may arise as coupled oscillations of small perturbations of the temperature and the electric field. They both theoretically and experimentally studied the dependence of the frequency of the oscillations on the magnetic sweep rate and the temperature for a granular superconductors. The experimental results for magnetothermal oscillations in the temperature $T = 3 \div 7$ K and magnetic field sweep rate $\dot{B}_e = 10 \div 45$ G/s ranges show that at low values of the applied field $B_e(t)$ there is slow temperature increase due to the small vortex avalanches establishing the critical state. Above certain threshold magnetic field, will appear temperature oscillations with the period t in the range $t \sim 10 \div 70$ s and its amplitude increasing in time. A flux jump occurs close to the Bean field accompanied by a temperature rise up to about 12 K with a characteristic time of the order of 1 s. The frequency of these oscillations is proportional to the magnetic field sweep rate \dot{B}_e .

Recently, it has been shown [37] that the local Joule heating due to planar defects or low-angle grain boundaries can cause thermal instabilities in a high- T_c coated conductors. It was shown that the thermal instabilities are more pronounced at lower temperatures and magnetic fields or under poorer gas cooling. The author have obtained the stability criterion for a planar defect in a thin film for a power-law voltage-current characteristics of the sample on the basis of calculation a steady-state heat balance equation. It has been pointed by Gurevich [37], also that the highly nonlinear voltage-current characteristics may cause strong disturbances of the electric field and dissipation with spatial size much larger than the defect size in the sample. Thus the resulting local hot spots near defects can trigger thermal instability in thin films. At sufficiently low electric fields E the voltage-current characteristics of type-II superconductors is highly nonlinear and differential conductivity σ is a function of the electric field E [38, 39]. The dependence σ of E at small values of the electric field E may considerably affect the critical state stability and the occurrence of the flux jumps in the sample [39]. As recently has been shown by Mints [10] that the nonlinear differential conductivity σ significantly affects the flux jumping process and therefore the first flux jump field B_j in the flux creep regime. In particular, the author derived a criterion for thermomagnetic flux-jump instability for the case of transverse geometry of thin films taking into account the nonlinear dependence of the background electric field on sample conduc-

tivity in the framework of Bean's critical state model. It was shown that the magnetic field sweep rate affects the instability. This effect is connected with the non-linear electric field dependence of $j(E)$ in the flux creep regime. The first flux jump field B_j decreases with increasing sweep rate field \dot{B}_e . As flux creep is relatively strong in high- T_c superconductors, one may expect it to have a significant influence on the critical state stability in these materials.

A detailed measurements have been performed by means a torque and SQUID magnetometer during magnetic field sweep rate by Monier and Fruchter [40] in a single crystal of the organic superconductor. They found an expression for the first flux jump field B_j for a cylinder sample assuming that the temperature in the sample is uniform. The obtained criterion for flux jumps for a nonlinear voltage-current characteristic in the dynamic approximation in a good agreement with a recent results of Mints [10]. It was shown that magnetothermal instabilities may be suppressed by an increase of heat transfer coefficient or the use of thin samples. The activation energy, the screening current density and its temperature derivative has been found from the dynamic relaxation measurements.

In the present paper, we shall investigate the magnetothermal flux jump instabilities of the critical state in conventional and high- T_c superconductors. We determine the flux jump field B_j and critical state stability criterion within the framework of Bean's model. To determine the flux jump field an analytical simulations of coupled equations for the magnetic $\vec{B}(\vec{r}, t)$ and electric $\vec{E}(\vec{r}, t)$ field inductions and temperature $T(\vec{r}, t)$ has been performed. The field of the first flux jumps B_j is calculated analytically by using the dynamic and the adiabatic approximations. The qualitative analysis of the magnetic flux jumps instabilities for superconductors will be provided.

§1. Flux jump instabilities

Let us suppose that at the initial moment of time, the magnetic field in the sample is uniform and equal to B_0 , after which the external field rises to some value B_e . With an increase of the external field B_e , the vortices penetrates the sample. The viscous flow of vortices inside the sample causes an electric field E which generates persistent currents near the sample surface, having a density $j \simeq j_c$ and power dissipation. This dissipation heats the sample which leads to further changes in the magnetic flux density and further increase the sample temperature locally decrease in the critical current density j_c . With a decrease j_c , the vortex lines penetrates the sample more deeply, more heat is released and new dissipation occurs thus resulting in a new increase of temperature T . Under certain conditions such a dissipative flux motion can cause magnetothermal instabilities.

Mathematical problem of theoretical study the dynamics of thermal and electromagnetic perturbations in a superconductor sample in the flux creep regime can be formulated on the basis of a system nonlinear diffusion-like equations for the thermal and electromagnetic field perturbations with account nonlinear relationship between the field and current in superconductor sample. The distribution of the magnetic flux density \vec{B} and the transport current density \vec{j} inside a superconductor is described by the equation

$$\text{rot}\vec{B} = \frac{4\pi}{c}\vec{j}. \quad (1)$$

When the penetrated magnetic flux changes with time, an electric field \vec{E} is generated inside the sample according to Faraday's law

$$\text{rot}\vec{E} = \frac{1}{c} \frac{d\vec{B}}{dt}. \quad (2)$$

The temperature distribution in superconductor is governed by the heat conduction diffusion equation

$$\nu(T) \frac{dT}{dt} = \nabla[\kappa(T)\nabla T] + \vec{j}\vec{E}, \quad (3)$$

Here $\nu = \nu(T)$ and $\kappa = \kappa(T)$ are the specific heat and thermal conductivity, respectively. The above equations should be supplemented by a current-voltage characteristics of superconductors, which has the form

$$\vec{j} = \vec{j}_c(T, \vec{B}) + \vec{j}(\vec{E}). \quad (4)$$

In general, the critical current density depends, on both the local magnetic field B and local temperature T , thus, the magnetic flux profile is determined by equation $j_c = j_c(B, T)$. C.P. Bean [2] has proposed the critical state model which successfully used to describe magnetic and transport properties of hard superconductors. According to this model the current density \vec{j} is equal to the critical current density \vec{j}_c and independent of magnetic field. In order to obtain analytical results of a set Eqs. (1)-(4), we suggest that j_c is independent on magnetic field B and use the Bean critical state model $j_c = j_c(B_e, T)$. We suppose that the critical current density j_c is linearly dependent on the local temperature

$$j_c(T) = j_0 - a(T - T_0). \quad (5)$$

where $a = j_0/(T_c - T_0)$; j_0 is the equilibrium current density; T_0 and T_c are the equilibrium and critical temperatures of the sample, respectively. The characteristic field dependence of $j(E)$ in the region of sufficiently strong electric field ($E \geq E_f$) can be approximated by the piece-wise linear function $j = \sigma_f E$; $\sigma_f = \eta c^2/B\Phi_0 = \sigma_n H_{c2}/B$ is the effective conductivity in the flux flow regime; η is the viscous coefficient, $\Phi_0 = \pi\hbar c/2e$ is the magnetic flux quantum, σ_n is the differential conductivity in the normal state, H_{c2} is the upper critical magnetic field, E_f is the boundary of the linear area in the voltage-current characteristics of the sample [41]. Notice, that in the flux flow regime the differential conductivity σ_f is approximately constant, i.e., independent on the electric field E .

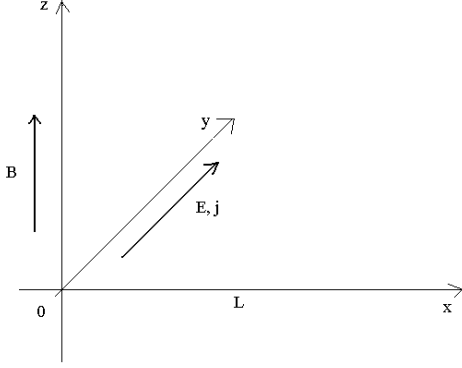


Fig.1 The geometry of the problem

Let us formulate a differential equations governing the dynamics of small temperature and electromagnetic field perturbation in a superconductor sample. We study the evolution of thermal and electromagnetic penetration process in a simple geometry - superconducting semi-infinite sample $x \geq 0$ (Fig 1.). We assume that the external magnetic field induction B_e is parallel to the z-axis and the magnetic field sweep rate \dot{B}_e is constant. When the magnetic field with the flux density B_e is applied in the direction of the z-axis, the transport current $j(x, t)$ and the electric field $E(x, t)$ are induced inside the slab along the y-axis. For this geometry the spatial and temporal evolution of small thermal $T(x, t)$ and electromagnetic field $E(x, t)$ perturbations are described by the thermal diffusion equation coupled to Maxwell's equations

$$\nu \frac{dT}{dt} = k \frac{d^2 T}{dx^2} + jE, \quad (6)$$

$$\frac{d^2 E}{dx^2} = \frac{4\pi}{c^2} \left[\frac{dj}{dE} \frac{dE}{dt} - \frac{dj_c}{dT} \frac{dT}{dt} \right]. \quad (7)$$

It should be noted that the nonlinear diffusion-type equations (6) and (7), totally determine the problem of the space-time distribution of the temperature and electromagnetic field profiles in the flux flow regime with a linear current-voltage characteristics in the semi-infinite sample.

The system of differential equations (6) and (7) may be integrated analytically subject to appropriate initial and boundary conditions for the thermal and electromagnetic small perturbations. We present the thermal boundary conditions as

$$\kappa \frac{dT(0, t)}{dx} = -w(T - T_0), \quad T(L, t) = T_0, \quad (8)$$

where w is the heat transport coefficient. Let us assume that the magnetic field perturbation is equal to zero at the sample surface and according to relation (2), we obtain the first electrodynamic boundary condition

$$\frac{dE(0, t)}{dx} = 0. \quad (9)$$

The second boundary condition for the electric field $E(x, t)$ at the flux front $x = L$ can be presented as

$$E(L, t) = 0, \quad (10)$$

The boundary conditions for the magnetic field induction are

$$dB(0, t) = B_e, \quad B(L, t) = 0,$$

where $L = \frac{cB_e}{4\pi j_c}$ is the London penetration depth.

§1.1. Dynamic instability

In this section we study the dynamics of flux-jump instability of during flux penetration into superconductor sample within the dynamical approximation [8]. As we know [8, 9] that a nature of the flux jumps depends on the competition between diffusive and dissipative processes through the dimensionless parameter

$$\tau = \frac{4\pi\sigma_f\kappa}{c^2\nu} = \frac{D_t}{D_m}.$$

where $D_t = \kappa/\nu$ is the thermal diffusivity and $D_m = c^2/4\pi\sigma_f$ the magnetic diffusivity coefficients, respectively. Therefore the flux instability criterion is determined mainly by the relation of the magnetic D_m and thermal D_t diffusion coefficients. Let us consider the case for the flux jumps corresponding to the limiting case $\tau \gg 1$. Consequently, it can be assumed that the initial rapid heating stage of a flux jump takes place on the background of a "frozen-in" magnetic flux. Therefore, under this dynamic approximation, we obtain from (7) the relation between electric field $E(x, t)$ and temperature $T(x, t)$ perturbations in the following form

$$\frac{dj}{dE} E - \frac{j_c}{T_c - T_0} T = 0 \quad (11)$$

We notice that the last relation between $E(x, t)$ and temperature $T(x, t)$ has been derived in the assumption that the decrease of the critical current density j_c resulting from a temperature perturbation $T(x, t)$ compensates with increase of the resistive current density j resulting from an electric field perturbation $E(x, t)$, so a total current density remains constant [8]. Upon substituting the expression (11) into the equation (6) and excluding the variable $E(x, t)$ one can get the differential equation for the distribution of thermal perturbation, which can be conveniently presented in the following dimensionless form

$$\frac{d^2\Theta}{dz^2} + \frac{d\Theta}{d\tau} + \delta\Theta = 0. \quad (12)$$

Here we introduced the following dimensionless variables

$$\Theta = \frac{T}{T_c - T_0}, \quad \tau = \frac{t}{t_k}, \quad t_k = \frac{\nu L^2}{\kappa}, \quad z = \frac{x}{L},$$

and parameters

$$E_e = \frac{aL^2}{\kappa}, \quad \delta = \frac{j_c}{\sigma_f E_e}.$$

The equation (12) can be easily solved by using a method of separation of variables. Taking into account the thermal boundary conditions

$$\Theta(1, \tau) = 1, \quad \frac{d\Theta(0, \tau)}{dz} = 0. \quad (13)$$

an explicit solution to equation (12) can be written as the following form

$$T(x, t) = (T_c - T_0) \exp \left[\left(\delta - \frac{\pi^2}{4L^2} \right) (t - t_0) \right] \cos \frac{\pi}{2L} x + T_0 \quad (14)$$

where t_0 is a constant parameter. The distribution of the electric field perturbation $E(x, t)$ can be found by using relations (11) and (14)

$$E(x, t) = E_c \exp\left(\left[\delta - \frac{\pi^2}{4L^2}\right](t - t_0)\right) \cosh \frac{\pi}{2L} x \quad (15)$$

Using the obtained solutions (14) and (15) one can easily find the critical field B_j starting from which flux jump takes place

$$B_j = \frac{\pi^2}{2} \left[16 \frac{\kappa}{a} \frac{\sigma_f j_c}{c^2}\right]^{1/2} \quad (16)$$

and the critical thickness d_c of the sample

$$d_c = \frac{\pi}{2} \sqrt{\frac{\sigma_f \kappa}{a j_c}}. \quad (17)$$

We can easily estimate B_j and d_c using by a typical numerical values of a well known parameters of the sample which has been made in many publications (see, for example [8]).

The dynamic approximation which we used here is justified if the thermal flux diffusion is much greater than the magnetic diffusion $D_t \gg D_m$. The thermal $D_t = 10^3 \div 10^4 \cdot \text{cm}^2/\text{s}$ and magnetic $D_m = 1 \div 10 \cdot \text{cm}^2/\text{s}$ diffusion coefficients we estimated using by a numerical values of parameters. On the other hand, using the obtained numerical values of D_t and D_m it is easily estimate the thermal and magnetic diffusion times, taking into account that, both t_κ and t_m are inversely proportional to the corresponding thermal and magnetic diffusion coefficients, respectively. Then one can be seen, within the time interval $t_\kappa \ll \Delta t \ll t_m$ the results obtained provide for a highly accurate description of the dynamical evolution of temperature and electromagnetic perturbations in the superconductor sample.

§1.2. Adiabatic instability

In the adiabatic approximation we assume that rapid propagation of the flux line is accompanied by an adiabatic heating of the superconductor [8]. In this case the thermal conditions have a little effect on the occurrence of the flux jumps. Therefore thermal conductivity is negligible and corresponding term can be neglected in the heat diffusion equation. In this limiting case $\tau \ll 1$ the distribution of the electric field is described by the following nonlinear equation

$$e \frac{d^3 e}{d\tau dz^2} - \frac{d^2 e}{dz^2} \frac{de}{d\tau} + \left[\left(\frac{de}{d\tau} \right)^2 - e \frac{d^2 e}{d\tau^2} \right] + e^2 \frac{d^2 e}{dz^2} = 0. \quad (18)$$

$$\tau = \frac{t}{t_m}, \quad t_m = \frac{L^2}{D_m}, \quad z = \frac{x}{L}, \quad e = \frac{E}{E_e}, \quad E_e = \frac{\sigma_f \nu}{a}.$$

The solution of (18) together with the boundary conditions (8) can be easily obtained analogously, as in a previous section, so we have

$$e(z, \tau) = \lambda(\tau) \psi(z). \quad (19)$$

after substituting the last relation into (18) one obtains the following expressions for the functions $\phi(x)$ and $\lambda(\tau)$

$$\frac{d^2 \phi}{dx^2} + k = 0, \quad (20)$$

$$f \frac{d^2 f}{d\tau^2} - \left(\frac{df}{d\tau} \right)^2 + k f^2 = 0, \quad (21)$$

where k is the constant parameter to be determined. The equation (20) has an explicit solution

$$\phi(x) = \frac{k}{2} (1 - z^2). \quad (22)$$

Let us rewrite the equation (21) in the form of

$$\left(\frac{df}{d\tau} \right)^2 = 2f^2 (b - kf). \quad (23)$$

which has an exact solution in the form

$$f(\tau) = \frac{b^2}{k} \text{ch}^{-2} \frac{b(\tau - \tau_p)}{\sqrt{2}}. \quad (24)$$

where τ_p is the integrating constant and b is the free parameter. Combining above solutions (22) and (24) we get the following expression for the electric field and temperature distribution

$$E(x, t) = \frac{E_e}{2} \frac{(L^2 - x^2)}{\text{ch}^2 \frac{b(t - t_p)}{\sqrt{2}}} \quad (25)$$

$$T(x, t) = \frac{\sigma_f E_e}{2a} (L^2 - x^2) \left[\text{ch}^{-2} \frac{b(t - t_p)}{\sqrt{2}} - 1 \right] + \sqrt{2} E_e \frac{b}{a} \frac{b(t - t_p)}{\sqrt{2}} + T_0. \quad (26)$$

According to (25) perturbation $E(x, t)$ decreases exponentially with time $\Delta t = \sqrt{2}/b$. Motion of flux lines caused by $E(x, t)$ perturbations leads to increase temperature in the region $x \leq L$ of the sample. From (26) at $t - t_p \gg \Delta t$ we obtain the following expression for the maximum heating during the flux jump

$$\Delta \Theta_m = \frac{T - T_0}{T_c - T_0} = 2 \sqrt{\frac{\sigma_f E_e}{j_c \beta}}. \quad (27)$$

Numerical estimation gives $\Delta \Theta_m \sim 2 \div 3$ for the typical values of parameters of the sample. Such amount of heating will be dissipated during the adiabatic flux jump instability which is determined by a well known stability parameter

$$\beta = \frac{4\pi L^2 j_c^2}{c^2 \nu (T_c - T_0)}. \quad (28)$$

A more detailed derivation of the adiabatic stability criterion for flux jumps within the framework of Bean critical state model has been given in [8]. To compare the theoretical value of β with experimental data, one must know the temperature dependence the heat capacity coefficient of the sample, which at low temperatures can be expressed as $\nu(T) \sim \nu_0 (T/T_0)^n$, where ν_0 is a numerical factor, $n \simeq 3.1$. Using the expression for $\nu(T)$ one can estimate the value of β numerically for an existing of various functional dependencies of $j_c(T)$. It should be noted that due to high values of critical temperature and thus heat capacity in high T_c superconductors, the experimental value of the first flux jump field β can be larger than in conventional type II superconductors.

§1.3. Flux creep

In general, the critical state stability threshold is determined by many external and internal factors, as by the sweep rate of the external magnetic field, the type of voltage-current characteristics, the critical current density and its magnetic field and temperature derivatives, the profile temperature and surface cooling conditions, the sample geometry and pinning properties of the considered sample. The obtained above results are valid in the flux flow regime, where voltage current-current characteristics of hard superconductor is described by linear dependence of $j(E)$ at sufficiently large values of electric field [41]. As can be seen from the obtained results for the flux flow state the value of B_j depends mainly on the critical current density and the specific heat of the sample. The nonlinear part of the curve $j(E)$ in the region of weak electric fields is associated with flux creep. In the flux creep regime the magnitude of flux jump field B_j strongly depends on variation of external parameters, in particular, on the magnetic field sweep rate [10, 11]. It can be shown [10, 11] that flux creep may sufficiently affect on the occurrence of the flux jump instabilities. In this section we shall discuss the effect of flux creep and the nonlinear current-voltage characteristics on the threshold of flux jumps, qualitatively. The current-voltage characteristics of type-II conventional as well as high- T_c superconductors in the flux creep regime is a highly nonlinear due to thermally activated magnetic flux motion. Thermally activated flux motion or flux creep problem in superconductor samples with various geometries and conditions has been recently extensively studied by many researchers [42-64]. According to Kim-Anderson theory [55, 56] the thermally activated flux motion is described by a well known expression

$$v = v_0 \exp[-U/kT], \quad (29)$$

Here v_0 is the velocity of the thermally activated flux motion at zero temperature, U is the activation energy due to vortex pinning. The activation energy $U = U(j, B, T)$ depends on temperature T , magnetic field induction B and current density j . The dependence of U on the current density j is extensively discussed in the literature [57]. In particular, Burlachkov et al. [58] have analyzed the flux creep at different dependencies of the activation energy U on field B and current density j . For the vortex glass and collective creep models the potential barriers highly nonlinear function of j [59]. A voltage-current characteristic of a type-II superconductor in the flux creep state is characterized by the power or exponential law increase of E with increasing j . For the linear current dependence of the potential barrier $U(j)$ [55, 56], the dependence $j(E)$ has the form

$$\vec{j} = j_c + j_1 \ln \left[\frac{\vec{E}}{E_c} \right], \quad (30)$$

where parameter j_1 determines the slope of the j-E curve and it is assumed $j_1 \ll j_c$. In this case the differential conductivity σ is determined by the following expression (see, Refs. [10, 11])

$$\sigma = \frac{dj}{dE} = \frac{j_1}{E}. \quad (31)$$

For the logarithmic current dependence of the potential barrier $U(j)$ proposed by Zeldov et.all. [59]

$$U(j) = U_0 \ln \left[\frac{j_c}{j} \right]^n, \quad (32)$$

the dependence $j(E)$ has the form

$$\vec{j} = j_c \left[\frac{\vec{E}}{E_c} \right]^{1/n}, \quad (33)$$

when the flux creep is determined by numerous spatial defects of the sample. $U_0 = \text{const}$ and E_c is the crossover electric field. Here the parameter $n = U_0/kT$ is a function of temperature T , magnetic field H and depends on the pinning regimes and can vary widely for various types of superconductors. In the case $n = 1$ the power-law relation (33) reduces to Ohm's law, describing the normal or flux-flow regime. For infinitely large n , the equation describes the Bean critical state model $j = j_c$ [1]. When $1 < n < \infty$, this equation describes nonlinear flux creep [59]. In this case the differential conductivity σ is determined by the following expression

$$\sigma = \frac{dj}{dE} = \frac{j_c}{nE}. \quad (34)$$

It is assumed, for simplicity, that the value of n temperature and magnetic-field independent. It should be noted that the nonlinear diffusion-type equations (6) and (7), completed by the flux creep equation (34), totally determine the problem of the space-time distribution of the temperature and electromagnetic field profiles in the flux creep regime with a nonlinear current-voltage characteristics in a semi-infinite superconductor sample.

It should be noted that the investigation of the stability conditions in the flux creep regime is very difficult due to absence of solution of system equations (6)-(7) together with nonlinear $j(E)$ dependence. However, in some limiting cases, it can be solved the problem if we take into account that the heating due to viscous flux motion is negligibly small and get some approximate solution, describing the evolution of thermal and magnetic field diffusion in the creep regime. According to relation (34) the conductivity decreases with the increasing of electric field E , while $\sigma \sim E^{-1}$ and it strongly depends on the external magnetic field sweep rate $E \sim \dot{B}_e$. Therefore the stability criterion also strongly depends on the differential conductivity σ [10].

§1.4. Dynamical approximation

For the small thermal $\delta T(x, t)$ and electromagnetic field $\delta E(x, t)$

$$\delta T = \Theta(x) \exp[\gamma t], \quad (35)$$

$$\delta E = \epsilon(x) \exp[\gamma t]. \quad (36)$$

perturbations the system of differential equations (6) and (7) can be written in the following form

$$\nu \gamma \Theta = \kappa \frac{d^2 \Theta}{dx^2} + j_c \epsilon, \quad (37)$$

$$\frac{d^2 \epsilon}{dx^2} = \frac{4\pi}{c^2} \gamma \left[\frac{j_c}{n E_b} \epsilon - \frac{j_c}{T_c - T_0} \Theta \right]. \quad (38)$$

where γ is the eigenvalue of the problem to be determined. It is clear that the rate γ characterizes the time development of the instability. In the case, when $\text{Re} \gamma \geq 0$, small thermal and electromagnetic perturbations increase and the stability margin corresponds to the case when $\gamma=0$. It should be noted that the nonlinear diffusion-type equations (37) and (38), totally determine the problem of the space-time distribution of the temperature and electromagnetic field profiles in the flux creep regime with a

nonlinear current-voltage characteristics in the semi-infinite sample.

As we have mentioned above, the differential conductivity $\sigma(E)$, which determines the dynamics of the instability is high in the flux creep regime and the parameter τ is high enough, also [10, 11]. It is clear that this picture for the flux jumps corresponds to the limiting case $\tau \gg 1$. Consequently, it can be assumed that the initial rapid heating stage of a flux jump takes place on the background of a "frozen-in" magnetic flux. Therefore, under this dynamic approximation, we obtain from (38) the relation between electric field $\epsilon(x, t)$ and temperature $\Theta(x, t)$ perturbations in the following form

$$\frac{j_c}{nE}\epsilon - \frac{j_c}{T_c - T_0}\Theta = 0 \quad (39)$$

Upon substituting the expression (39) into the equation (37) one can easily get a differential equation for the temperature distribution, which is conveniently presented in the following dimensionless form

$$\frac{d^2\Theta}{d\rho^2} - \rho\Theta = 0. \quad (40)$$

Here we introduced the following dimensionless variables

$$\rho = \frac{\gamma - z}{r}, \quad z = \frac{x}{L}, \quad \frac{1}{r} = \left[n \frac{aL^2}{\kappa} E_L \right]^{1/3}, \quad E_L \sim \dot{B}_e.$$

Thus, the condition of existence of a non-trivial solutions of equation (40) allows to determine the spectrum of eigenvalues of γ and the instability threshold, accordingly. The equation (40) has an exact solution in terms of Airy functions given as the following form

$$\Theta(\rho) = c_1(s)Ai(\rho) + c_2(s)Bi(\rho). \quad (41)$$

where $Ai(\rho)$ and $Bi(\rho)$ are the Airy functions. Here constants of integration c_1 and c_2 are determined from the thermal boundary conditions. Substituting the last solution (41) into the thermal boundary conditions we find that $c_2 = 0$ and $\Theta(\rho) = c_1(s)Ai(\rho)$. Applying the second boundary condition we get an equation to determine the eigenvalues of the problem

$$J_{2/3}(a_n) = J_{-2/3}(a_n).$$

where a_n are the zeros of the Bessel function, which grows with increasing n . For example, for $n=1$ the stability criterion is presented as

$$a_1 = r^{2/3}\gamma. \quad (42)$$

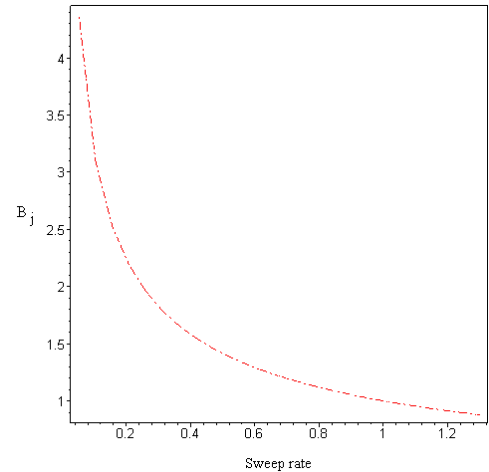
Using the value for the magnetic field penetration depth, we can easily obtain from (42) an expression for the threshold magnetic field B_j at which the flux jump occurs

$$B_j = \frac{4\pi j_c}{c} \sqrt{\frac{\kappa}{anE_L}}. \quad (43)$$

Let us now estimate the threshold field for a typical values of parameters $j_c \simeq 10^9 A/m^2$, $T_c - T_0 \simeq 10$ K, $\kappa \simeq 10^{-1} W/Km$, $n=10$. The background electric field $E_L \simeq \dot{B}_e L$, induced by the magnetic-field variation $\dot{B}_e \simeq 10^{-2} \div 10^{-3}$ T/s is of the order of $E_L = 10^{-4} \div 10^{-5}$ V/m for the value of $L = 0.01$ m. We can easily estimate that the threshold field has the value $B_j \simeq 1 \div 3T$.

Experimentally, the background electric field E_L is created by the sweeping rate of the applied magnetic field \dot{B}_e . As can

be seen from the relation (43) the threshold field B_j is decreased with the increasing of background electric field E_L . It is noticeable that the dependence of the flux-jump field B_j on the sweeping rate \dot{B}_e of the applied magnetic field have been verified by a numerous experiments [15-21]. An intensive numerical analysis on the sweep rate dependence of the threshold field has been performed recently in [22]. Recent magnetization measurements [17] have shown that the value of the threshold field B_j decreases as the sweep rate \dot{B}_e increases. A theoretical investigations on the dependence of threshold field on the varying external magnetic field has been performed by many researchers (see, for example Ref. [8]). Within the framework of the flux jump instability theory, a rapid variation of the applied magnetic field acts as the instability-driving perturbation, and that threshold field B_j should decrease with increasing the sweeping rate \dot{B}_e [8]. The numerical studies [22] have demonstrated that the flux jumps takes place when the sweep rate \dot{B}_e increases up to a certain value, where the number of jumps increases with the sweep rate \dot{B}_e . As the sweep rate further increases, these simulation results show that the flux-jump field decreases and approaches a saturation value, which is fairly close to the experimental value of about 10^2 Oe [17]. However, as has been mentioned in [17], an experimental investigations on the dependence of the threshold field for the flux jump field B_j on the external magnetic field sweep rate \dot{B}_e is very little. Experimentally, can be observed a complex behavior of dependence of the threshold field B_j on the sweep rate \dot{B}_e . The results of experiments of Ref. [17] demonstrated that B_j is independent of the sweep rate in a defined range of temperatures. Thus, the near independence of B_j on the sweeping rate remains to be explained. In some conventional superconductors both the independence of B_j on the sweeping rate and its growth at a high sweeping rate [17-19] were detected. It has been suggested [9] that a nonuniform heating may be responsible for such an effect. However, theoretical understanding of the thermomagnetic instabilities at such conditions is still lacking. Note, however, that some details of the local field behavior depend indeed on the sweeping rate, as, for example, the number and amplitude of the jumps. In [22], it has been demonstrated that at low values of the sweep rates \dot{B}_e the number of flux jumps decreases as sweep rate increases. At still high sweep rates the amplitude of flux jumps becomes independent of the sweep rate and saturates to the limit with further increasing sweep rate.



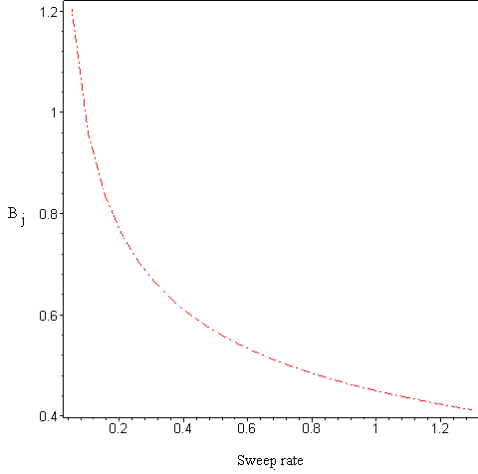


Fig. 2 and 3. The sweep rate dependence of the threshold field

In Fig. 2 and 3 we have demonstrated the dependence of the threshold field B_j on the external magnetic field sweep rate at $B_j \sim \dot{B}_e^{-1/2}$ and $\sim \dot{B}_e^{-1/3}$, respectively. As can be seen, the value of B_j decreases as the sweep rate increases. As the sweep rate increases the value of B_j decreases and it tends to saturate at high sweep rates. Magnetic field dependence of the critical current density only slows down the decrease of the field B_j with increasing external magnetic field sweep rate [10, 11]. We note that for the case Kim-Anderson model [55], the absolute value of the exponent in the power formula decreases from 1/2 to 1/3, so $B_j \sim \dot{B}_e^{-1/3}$ [10].

Thus, the stability criterion for the flux jumps demonstrates extremely high sensitivity of the threshold field B_j on the values of the critical current density j_c , thermal conductivity κ , and its external magnetic field sweep rate \dot{B}_e . It follows from above criterion that the value of the threshold field B_j is inversely proportional to the square root of the magnetic-field sweeping rate \dot{B}_e . Therefore, with the increase of sweeping rate \dot{B}_e the threshold field B_j decreases, as can be seen from Figures 2 and 3.

§1.5. Adiabatic approximation

Let us now study the space and time evolution of small thermal and electromagnetic perturbations within adiabatic approximation, taking into account nonlinear flux problem. To find an analytical solution of equations (6) and (7) we use simple adiabatic approximation, assuming that $\tau \ll 1$. Then eliminating the variable $\Theta(x, t)$ by using the relationship (6) and substituting into (7), we obtain a second-order differential equation for the distribution of small electromagnetic perturbation $\epsilon(x, t)$ in the form

$$\frac{d^2 \epsilon}{dz^2} = \epsilon^\gamma \frac{d\epsilon}{d\tau} - \beta \epsilon. \quad (44)$$

Here, we introduced the following dimensionless variables

$$z = \frac{x}{L}, \quad \tau = \frac{t}{t_0}, \quad \epsilon = \frac{E}{E_c}, \quad t_0 = \frac{4\pi j_c L^2}{c^2 E_c}, \quad \gamma = \frac{1-n}{n}.$$

Since we have neglected the redistribution of heat in deriving (44), only, electrodynamic boundary conditions should be imposed on this equation

$$\epsilon(1, \tau) = 0, \quad \frac{d\epsilon(0, \tau)}{dz} = 0. \quad (45)$$

An explicit solution of (44) together with the boundary conditions (45) can be obtained by using the method of separation of variables. Looking for the solution of equation (44) in the form

$$\epsilon(z, \tau) = \lambda(\tau)\psi(z). \quad (46)$$

we get the following expressions for a new variables

$$\frac{d\lambda}{d\tau} = -k\lambda^{1-\gamma}, \quad (47)$$

$$\frac{d^2 \phi}{dz^2} = k\phi^{\gamma+1} - \beta\phi. \quad (48)$$

By integrating equation (47) we easily obtain

$$\lambda(\tau) = (\tau_p - \tau)^{-1/\gamma}, \quad (49)$$

where τ_p is the constant parameter, describing the characteristic time of magnetic flux penetration profile; $k = 1/\gamma$. Now, integrating twice, the ordinary differential equation for the function $\phi(z)$ with the boundary conditions (45) and taking into account (49), we find the following explicit solution for the electromagnetic field distribution

$$\epsilon(z, \tau) = \left[\frac{D}{\tau_p - \tau} \cos^2 \frac{2\pi}{L^*} z \right]^{1/\gamma}, \quad (50)$$

$$D = \frac{n^2}{1-n^2} \frac{\beta}{2}, \quad L^* = \frac{1-n}{n} \frac{\pi}{\sqrt{\beta}},$$

The obtained solution (50) describes the distribution of the electromagnetic field in the flux creep regime with a power-law current-voltage characteristics. The solution describes an blow-up-type instability in the superconductor sample. As easily can be seen that the solution remains localized within the limited area $x < L^*/2$ with increasing infinitely of time. In other words, the growth of the solution, becomes infinite at a finite time τ_p . Typical distributions of the electric field $\epsilon(z, t)$ determined from analytical solution (50) is shown in Figure 1 for the values of parameters $\tau_p=1, n=2, \beta \sim 1$ and $L^* \sim 0.01$.

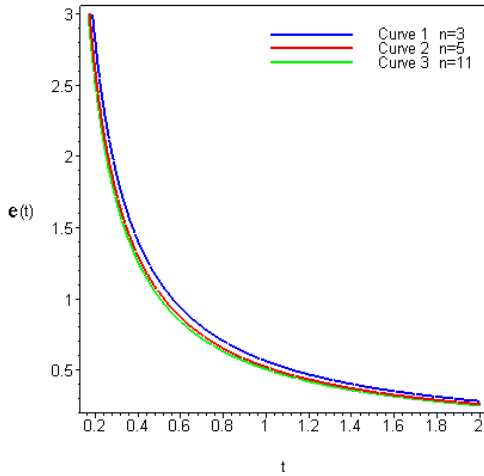
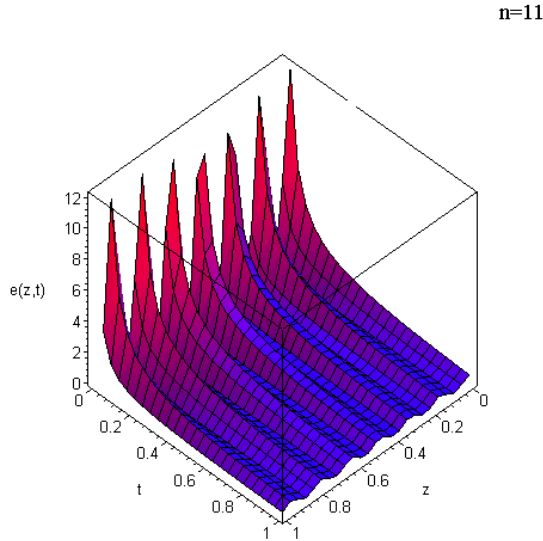
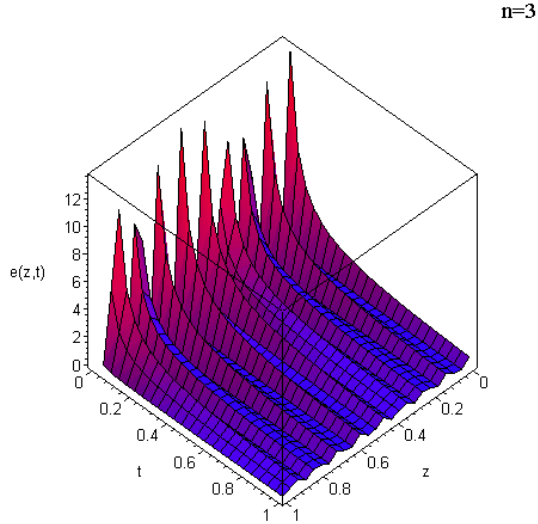


Fig.4a-4b. The space and time evolution of the electric field

profile at different times for $\tau_p=1$, $n=2$, $\beta \sim 1$ and $L^* \sim 0.01$.

Fig.4c. The time evolution of the electric field profile at $\tau_p=1$, $n=2$, $\beta \sim 1$ and $L^* \sim 0.01$.

Notice, that for the Kim-Anderson model the solution of the flux creep problem has the form

$$\epsilon(z, \tau) = \frac{1}{\beta(\tau - \tau_0)} \left[\cos\left(\frac{2\pi}{L} \sqrt{\beta x}\right) + 1 \right]. \quad (51)$$

Alternatively, this solution can be obtained from (50) in the limiting case, when $n \rightarrow \infty$.

§1.6. Nonuniform temperature profile

It is important to notice that the profile of temperature $T(x, t)$ may also significantly influence the condition of occurrence of flux jumps in superconducting sample. In many cases in studying the dynamics of thermal instabilities of superconductors were usually assumed that the spatial distribution of temperature is homogeneous in the cross section of the sample. However, in reality, the temperature profile of superconductor may be inhomogeneous along the sample as well as in its cross sectional plane. Such inhomogeneities can appear due to different physical reasons. First, the vortex structure can be inhomogeneous due to existence of weak bonds in the sample. Second, the inhomogeneities may be caused by the dependence of the critical current density on magnetic field, the differential conductivity and the heat conductivity. It has been recently shown [65] that under the quasi-adiabatic conditions the temperature profile can be essentially inhomogeneous, which strongly affects the stability criterion of the critical state of superconductors and the first flux jump field.

In this section we develop a phenomenological description of flux jumps in the presence of a temperature gradient and electric field in hard superconductors. It has been shown that thermoelectric effects can significantly influence the stability conditions in the mixed state of superconductors at very low temperatures. Theoretical and experimental investigations show [66-79] that in the mixed state during the motion of vortices inside the superconductor sample may occur thermoelectric effects - temperature gradients. Under certain conditions the presence of a temperature gradient in type II superconductor sample leads to critical state instabilities. Many investigations have been carried out on the thermoelectric effects in type-II superconductors, as well as in high- T_c superconductors both experimentally and theoretically [66-79]. The discovery of high- T_c superconductors stimulated intensive study of the transport phenomena caused by the flux-flow under an electrical current and temperature gradient. In the presence of temperature gradient ∇T an additional thermal force appears in the sample due to the existence of a transport entropy of vortex lines

$$F_t = -s\nabla T, \quad (52)$$

where $s = s(T)$ is the transport entropy of a vortex line [79]

$$s = s_0(T/T_c)(1 - T/T_c). \quad (53)$$

Here s_0 is the entropy density neglecting the transport entropy of the flux lines. It is noticeable that the existence of the transport entropy s is associated with the presence of low-energy electron states localized in the core of vortices and the value of s can be approximated from the local density of states [78, 79]

$$s \sim \frac{m_e^{3/2} \epsilon_f^{1/2} \xi^2}{h^3} k_B^2 T. \quad (54)$$

Here ϵ_f is the Fermi energy, k_B is the Boltzmann constant, ξ is the coherence length.

The critical state equation with an account the transport entropy has the form

$$\vec{j} = \vec{j}(T, \vec{H}, \vec{E}) + S \nabla T, \quad (55)$$

where $S = \frac{sc}{\Phi_0}$. An additional heat released due to the transfer of transport entropy by a vortex lines, which is proportional to S . Then the equation to heat flux density \vec{q} can be written as

$$\vec{q} = -\kappa \nabla T + \frac{ST}{B} [\vec{E}, \vec{B}]. \quad (56)$$

In the quasi-stationary approximation, terms with time derivatives can be neglected in Eqs. (1)-(3). This means that the heat transfer from the sample surface compensates the energy dissipation arising in the viscous flow of magnetic flux in the system with an effective conductivity σ_f . In this approximation, the solution to equation (2) has the form

$$E = \frac{\dot{B}_e}{c} (L - x). \quad (57)$$

Upon substituting the expression (55) and (57) into (6), we get an inhomogeneous equation for the temperature distribution

$$\frac{d^2 \Theta}{d\rho^2} - \mu \rho \frac{d\Theta}{d\rho} - \rho \Theta = f(\rho). \quad (58)$$

Here we introduced the following dimensionless variables

$$f(\rho) = -[1+r\alpha\rho] \frac{j_c}{aT_0}, \quad \Theta = \frac{T - T_0}{T_c - T_0}, \quad \rho = \frac{L - x}{r}, \quad \omega = \frac{\sigma_f \dot{B}_e}{c j_c},$$

$$\mu = \frac{s_0 \dot{B}_e L^2 r^2}{c\kappa}, \quad r = \left[\frac{c\kappa}{a \dot{B}_e L^2} \right]^{1/3}.$$

Taking into account the thermal boundary conditions (8) an exact solution to equation (58) is obtained

$$\Theta(y) = \exp \left[\frac{y^2}{4} - \frac{\rho}{\mu} \right] [C_1 D_\eta(y) + C_2 D_{-\eta-1}(y) + \Theta_0(y)], \quad (59)$$

$$\begin{aligned} \Theta_0(y) &= -\frac{2\pi}{\Gamma(-\eta)} D_\eta(y) \int_0^y f(y') y' D_{-\eta-1}(y') dy' \\ &+ \frac{2\pi}{\Gamma(-\eta)} D_{-\eta-1}(y) \int_0^y f(y') y' D_\eta(y') dy', \\ y &= \mu^{1/2} \left[\rho + \frac{2}{\mu^2} \right], \quad \eta = \mu^{-3}, \end{aligned}$$

where C_1 and C_2 are integration constants, which are determined with the help of the thermal boundary conditions. In order to estimate the maximum temperature in the sample we present a solution to (58) in the form

$$\Theta(x) = \Theta_m - \rho_0 \frac{(x - x_m)^2}{2}.$$

near the point at which the temperature is a maximum, $x = x_m$. Substituting the last relation into equation (58) we obtain an expression for the maximum heating due to magnetic flux jumps

$$\Theta_m = \frac{\left[j_c + \frac{\sigma_f \dot{B}_e}{c} (L - x_m) \right] \frac{\dot{B}_e}{c\kappa T_0} (L - x_m)}{\frac{\gamma}{L^2} - \frac{\dot{B}_e}{c\kappa} (L - x_m) \left[\frac{s_0 \gamma}{2L^2} (2x_m - L) + a \right]}, \quad (60)$$

where $\gamma \sim 1$. The calculation of the maximum heating is demonstrated that in the isothermal case, when the sample surface is cooled intensively $w = w_0 L / \kappa \gg 1$ it is easy to verify that the maximum heating is considerably small $\Theta_m \ll 1$ for the typical values of physical parameters. In the case of weak sample cooling $w \ll 1$ the maximum heating is about $\Theta_m \approx 0,5 \div 2$. On the other hand, the analysis of solution (58) show that their contribution is small in the region of $x_m \leq x \leq L$ due to the of small amplitude of the background electric field $E = \dot{B}_e(x - x_m)/c$. On the other hand, near the point $x = x_m$ the temperature gradient dT/dx is comparatively small. Therefore, thermoelectric effects can significantly change the temperature profile in the critical state of the sample at the surface layer $0 \geq x \geq x_m$ only, where the background temperature gradients and the background electric field are greater. Near the point of $x = x_m = L/2$ thermoelectric effects are absent. The dimensionless transport entropy parameter μ can be presented in the form

$$\mu = \frac{s_0}{aL} \left[\frac{aB_e^2}{4\pi\nu j_c} \frac{\dot{B}_e t_\kappa}{B_e} \right]^{1/3}. \quad (61)$$

It is easily seen that $\mu \sim 1$ near the threshold for a flux jump, when $\frac{aB_e^2}{4\pi\nu j_c} \sim 1$ and $\frac{\dot{B}_e t_\kappa}{B_e} \sim 1$. The temperature rise during the flux jump depends mainly on the sweep rate of the external magnetic field and heat capacity and thermal conductivity parameters in the sample. As seen the temperature dependence $\mu(T)$ is determined by the relationship $t_\kappa = \frac{\nu L^2}{\kappa(T)}$. At low temperatures the transport entropy increases with temperature as

$$\mu(T) \sim s_0 T^{-1/3}, \quad (62)$$

because $\kappa \sim T$. This means that the influence of the thermoelectric effects on characteristics of the critical state stability in the sample can be significant under extremely low temperatures ($T \leq 0,1$ K). Unfortunately, quantitative data for the transport entropy coefficient s_0 are available only in limited temperature intervals thus the exact numerical evaluation of μ proves to be difficult.

Let us investigate the stability of the critical state with respect to small thermal δT and electromagnetic δE fluctuations with an account thermoelectric effects in the quasi-stationary approximation. We present solutions to Eqs. (1)-(4) in the form

$$T(x, t) = T(x) + \exp \left\{ \frac{\lambda t}{t_\kappa} \right\} \Theta \left(\frac{x}{L} \right), \quad (63)$$

$$E(x, t) = E(x) + \exp \left\{ \frac{\lambda t}{t_\kappa} \right\} \epsilon \left(\frac{x}{l} \right),$$

where $T(x)$ and $E(x)$ are solutions to the unperturbed equations obtained in the quasi-stationary approximation describing the background distributions of temperature and electric field in the sample and λ is the eigenvalue of the problem to be determined. The instability region is determined by the condition that $\text{Re} \lambda \geq 0$. From solution (63), one can see that

the characteristic time of thermal and electromagnetic perturbations t_j is of the order of t_κ/λ . Linearizing Eqs. (6)-(7) for small $\Theta/T(x), \epsilon/E(x) \ll 1$ perturbations we obtain the following equations in the quasi-stationary approximation

$$\begin{aligned} \nu\lambda\Theta &= \kappa \frac{d^2\Theta}{dx^2} + s_0 E \frac{d\Theta}{dx} + [j + \sigma_f E] \epsilon - aE\Theta, \\ \frac{d^2\epsilon}{dx^2} &= \frac{4\pi\lambda}{c^2} \left[\sigma_f \epsilon - a\Theta + s_0 \frac{d\Theta}{dx} \right]. \end{aligned} \quad (64)$$

Eliminating the variable ϵ between two equations in (64), we obtain a fourth-order differential equation for the temperature distribution

$$\begin{aligned} \frac{d^4\Theta}{dz^4} - \left[2\frac{1}{f} \frac{df}{dz} - \eta \right] \frac{d^3\Theta}{dz^3} - [\lambda(1+\tau) + \phi - 2\frac{d\eta}{dz} + 2\frac{1}{f} \frac{df}{dz} \left(\eta - \frac{df}{dz} \right) + \\ \frac{1}{f} \frac{d^2f}{dz^2}] \frac{d^2\Theta}{dz^2} - [2\frac{d\phi}{dz} + 2\frac{1}{f} \frac{df}{dz} \left(\lambda + \phi + \frac{d\eta}{dz} \right) - \eta \frac{1}{f} \frac{d^2f}{dz^2} - 2\eta \left(\frac{1}{f} \frac{df}{dz} \right)^2 + \\ \lambda\tau \left[\eta - \frac{1}{\sigma_f E} \frac{d\eta}{dz} \frac{df}{dz} \right]] \frac{d\Theta}{dz} - [2 \left(\frac{1}{f} \frac{df}{dz} \right)^2 (\lambda + \phi) - \frac{1}{f} \frac{d^2f}{dz^2} (\lambda + \phi) - \\ 2\frac{1}{f} \frac{df}{dz} \frac{d\phi}{dz} + \left[\frac{f\phi}{\sigma_f E} - \lambda - \phi \right]] \Theta = 0. \end{aligned}$$

Here, we introduced the following dimensionless variables and parameters

$$\begin{aligned} z = \frac{x}{L}, \quad f(z) = j(z) + \sigma_f E(z), \quad \phi(z) = \frac{E(z)}{E_\kappa}, \quad \eta(z) = \frac{E(z)}{E_\eta}, \\ \nu = \nu_0 \left(\frac{T}{T_0} \right)^3, \quad \kappa = \kappa_0 \left(\frac{T}{T_0} \right), \quad E_\eta = \frac{\kappa}{s_0 L^2}. \end{aligned}$$

Let us first consider the development of thermomagnetic instability in the adiabatic approximation, which is valid for hard superconductors with $\tau \ll 1$. In this limiting case, as seen from (63), the characteristic times t_j of temperature and electromagnetic field perturbations have to satisfy the inequalities $t_\kappa \gg t_j \gg t_m$ and $\lambda\tau \ll 1$ or $\lambda \gg 1$. Using this approximation we reduce the last equation to a second order differential equation

$$\frac{d^2\Theta}{dz^2} + 2\frac{1}{f} \frac{df}{dz} \frac{d\Theta}{dz} + \left[2 \left(\frac{1}{f} \frac{df}{dz} \right)^2 - 2\frac{1}{f} \frac{d^2f}{dz^2} \right] \left[1 + \frac{\phi}{\lambda} \right] - \lambda\tau \Theta = 0. \quad (65)$$

Using the substitution

$$y = \int_0^z f^2(z) dz, \quad (66)$$

equation (65) can be rewritten in the following form

$$\frac{d^2\Theta}{dy^2} - \left(\frac{1}{f} \frac{d^2f}{dy^2} \left[1 + \frac{\phi}{\lambda} \right] - \frac{\lambda\tau}{f^4} \right) \Theta = 0. \quad (67)$$

Multiplying equation (67) by Θ and integrating the result with respect to y over the interval

$$0 \leq y \leq y_1 = \frac{1}{L} \int_0^{y_1} f^2(y) dy,$$

we easily obtain

$$\begin{aligned} \lambda\tau \int_0^{y_1} \frac{1}{f^4} \Theta^2 dy - \int_0^{y_1} \frac{1}{f} \frac{d^2f}{dy^2} \Theta^2 dy - \frac{1}{\lambda} \int_0^{y_1} \frac{\phi}{f} \frac{d^2f}{dy^2} \Theta^2 dy = \\ = \int_0^{y_1} \left(\frac{d\Theta}{dy} \right)^2 dy \end{aligned} \quad (68)$$

where we have used the equality

$$\int_0^{y_1} \frac{d^2\Theta}{dy^2} \Theta dy = \Theta(y) \left(\frac{d\Theta}{dy} \right) - \int_0^{y_1} \left(\frac{d\Theta}{dy} \right)^2 dy = - \int_0^{y_1} \left(\frac{d\Theta}{dy} \right)^2 dy \quad (69)$$

and boundary conditions. The right-hand side of Eq. (68) has a minimum at $\lambda = \lambda_c$:

$$\lambda_c = \sqrt{\tau} \left[\frac{\left| \frac{1}{f} \frac{d^2f}{dy^2} \right|_{min}}{|f^4|_{max}} \right]^{1/2}. \quad (70)$$

Now we try, to obtain an integral estimation of the increment λ , upper and lower limits of its occurrence. The behavior of the integrand in (70) is basically determined by the factor $E = \frac{\dot{B}_e L}{c} (1-z)$, which is equal to zero at $z = 1$ (the other factors change more smoothly). Hence, the integrand reaches its maximum at $z = 0$ and the upper estimate for λ_c is

$$\lambda_c \leq f[j(0), T(0), E(0)] \times 1.$$

It is evident that $\lambda_c \gg 1$ and $\lambda_c \tau \ll 1$ at $\tau \ll 1$. Numerical evaluation gives $\lambda_c \approx 10 \div 10^2$ at $\tau = 10^{-3}$. Equations (68) and (71) enable one to write the instability occurrence criterion in the form

$$\int_0^{y_1} \frac{1}{f} \frac{d^2f}{dy^2} n_T^2 dy \geq \frac{\pi^2}{y_1^2} + 2\sqrt{\tau} \left[\frac{\left| \frac{1}{f} \frac{d^2f}{dy^2} \right|_{min}}{|f^4|_{max}} \right]^{1/2}. \quad (71)$$

Here we introduced a normalized unit vector

$$n_T^2 = \frac{\Theta^2}{\int_0^{y_1} \Theta^2 dy}, \quad \int_0^{y_1} n_T^2 dy = 1 \quad (72)$$

and used the inequality

$$\int_0^{y_1} \left(\frac{d\Theta}{dy} \right)^2 dy \geq \frac{\pi^2}{4} \int_0^{y_1} \Theta^2 dy \quad (73)$$

which has been obtained with the help expansion of the function $\Theta(y)$ in Fourier's series

$$\Theta(y) = A_m \cos \frac{y(2m+1)\pi}{2}. \quad (74)$$

As can be easily seen that the shape of inequality (71) essentially depends on the type of coordinate dependence of the functions $j(y)$ and $f^{-1}(y)$. On the other hand, terms which is proportional $\sqrt{\tau}$ in (70) can be as significantly small in the limit $\tau \ll 1$. So, taking into account (74) and above mentioned suggestions, the inequality (71) can be rewritten in the form of

$$\int_0^{y_1} \frac{1}{f} \frac{d^2 f}{dy^2} n_T^2 dy \geq \frac{\pi^2}{y_1^2}. \quad (75)$$

The last inequality it may be intensify to the left-hand by using the relationship

$$\left[\int_0^{y_1} \frac{1}{f} \frac{d^2 f}{dy^2} n_T^2 dy \right] \leq \left[\int_0^{y_1} \left| \frac{1}{f} \frac{d^2 f}{dy^2} \right|^p dy \right]^{1/p} \left[\int_0^{y_1} |n_T^2|^{p/(p-1)} dy \right]^{(p-1)/p}$$

$$\left[\int_0^{y_1} \left| \frac{1}{f} \frac{d^2 f}{dy^2} \right|_{max}^p dy \right]^{1/p} \times 1 = \int_0^{y_1} \frac{1}{f} \frac{d^2 f}{dy^2} dy.$$

Thus, the last stability criterion can be written in the form

$$\int_0^{y_1} \frac{1}{f} \frac{d^2 f}{dy^2} dy \geq \frac{\pi^2}{y_1^2}. \quad (76)$$

The integral criterion for the critical state instability (76) unlike the analogous criterion for a homogeneous temperature profile, takes into account the influence of each part of the sample and therefore temperature gradients on the threshold for occurrence of flux jumps. Similar results can be found for the case of composite superconductors ($\tau \gg 1$) when instability develops under a frozen-in conditions of magnetic diffusion.

§2. Branching flux instabilities

The dynamics of vortices in type-II superconductors exhibits a wide variety of instabilities of thermomagnetic origin. Nonuniform magnetic flux penetration in superconductors, creating finger and dendritic patterns, has recently attracted considerable interest. It is generally accepted that the nonuniform penetration of the magnetic flux is a thermomagnetic effect due to the local overheating produced by the dissipative motion of vortices. As a consequence of the increased local temperature, the pinning barrier is lowered, leading to a large-scale flux invasion and to a final nonuniform magnetic flux distribution. Such dendritic type patterns driven by the flux jumping instability have been directly observed under a wide variety of conditions in a large number of superconducting samples by Duran et al. [80] and Vlasko-Vlasov et al. [81] in Nb films, by Johansen et al. [82], Bobyl et al. [83], Barkov et al. [84] in MgB₂, Leiderer et al. [85] in other superconducting materials by Bolz et al. [86, 87], Welling et al. [88] and Rudnev et al. [89] by means a magneto-optical imaging with a high spatial and temporal resolution. The existing experimental data [80-89] and the recently developed theoretical models [90-93], suggest that the origin of these patterns is thermomagnetic instability of the vortex matter in the superconducting films.

The above mentioned irregular flux avalanches and dendritic-like patterns has a threshold applied field and temperature, when the first avalanche occurs B_{th} , which strongly depends on both temperature and the sample size, as in conventional uniform flux jump instabilities [8-11]. The recently observed very much like some snow-avalanches - huge compact avalanches by Welling et al. [88] in Nb thin films by magneto-optical experiments also has a thermomagnetic origin as proposed by Aranson et al. [91]. The authors have determined the first flux jump field B_j as a function of temperature T and found that with increasing temperature more branching of the avalanches resulting in a more irregular flux pattern. At higher temperatures, the number of

avalanches decreases and more flux penetration starts to dominate the behavior. However, above certain temperature these flux avalanches were absent. Bolz et al. [87] have studied the dendritic flux patterns in superconducting YBCO films by means a combination of magneto-optics and pulsed laser irradiation with high spatial and temporal resolution in the micrometer and nanosecond ranges. They found that dendrites only develop for certain values of the external field and temperature. Bobyl et al. [83] have detected in their magneto-optical experiments both mesoscopic with the smallest size ($50\Phi_0$ at $B_e=4$ mT) and the macroscopic of dendritic shape with the large size ($10^6\Phi_0$ at $B_e=9$ mT) flux jumps in MgB₂ films. The results of their magneto-optical experiments have shown that the jump size increases with increasing of the applied field B_e . Both types of jumps disappear above the threshold temperature ($T=10$ K) due to fast increase of the specific heat and decrease of the critical current. The authors believed that both types of jumps has a thermomagnetic origin and its existence can be explained due to strong demagnetization effects in thin films. Barkov et al. [84] believed that the dendritic structures can be observed in thin films with a sufficiently small thickness and in an adiabatic conditions, when the heat diffusivity is much smaller than the magnetic diffusivity. They experimentally measured a value of threshold field B_j in a superconducting thin MgB₂ films using magneto-optical imaging technique which in well agreement with the existing theoretical data [8, 9]. It is known, that dendrite propagation in thin films shows velocities up to 160 km/s [86], i.e., these velocities are much higher than the speed of sound. Wertheimer and Gilchrist discovered a well defined pattern of flux dendrites with a propagation velocity v in the interval between 5 m/s and 100 m/s [94]. The dendrites velocity depends on the disks thickness, for smaller d a higher velocity was found. Bolz et al. [86] have found that for thin superconducting films the flux jump instability can give rise to dendritic magnetic flux avalanches propagating with tip velocities as high as 50 km/s. The dendritic type of flux penetration into type-II superconductor slab was proposed by Aronson and his co-workers [91] on the basis of numerical simulations of coupled equations for the magnetic induction and temperature in the limit of weak Joule heating in the sample. A formation of such dendritic flux front patterns can be observed under condition that the magnetic flux diffusion is much faster than the heat diffusion. They proposed that each vortex microavalanche results in a partial flux penetration process which is accompanied by local Joule dissipation. It has been pointed also that the dendritic microavalanches may be also initiated by macroscopic surface defects, which can trigger a global flux jump instabilities in high- T_c superconductors.

§2.1. Flux flow

Let us consider the problem of occurrence branching instabilities in the flux flow regime. For this purpose we formulate a basic equation governing the dynamics of magnetic field induction and temperature perturbation in a semi-infinite superconducting sample $x \geq 0$. The distribution of the magnetic flux density \vec{B} and transport current density \vec{j} inside a superconductor is given by a solution of the equation

$$\frac{dB}{dx} = \mu_0 j_c. \quad (77)$$

The electric field $E(x, t)$ is generated inside the sample according

to Faraday's law

$$\frac{dE}{dx} = \frac{dB}{dt}. \quad (78)$$

In the flux flow regime the electric field $E(x, t)$ induced by the moving vortices is related with the local current density $j(x, t)$ by the nonlinear Ohm's law

$$E = \rho(j - j_c). \quad (79)$$

Let us suppose that in the flux flow regime the differential resistivity is approximately constant and independent on magnetic field, i.e. $\rho = \rho_f = \text{const}$ [41]. The spatial and temporal evolution of thermal $T(x, t)$ and magnetic field $B(x, t)$ perturbations are described by the thermal diffusion equation coupled to Maxwell's equations

$$\begin{aligned} \frac{d\Theta}{dt'} &= \tau \frac{d^2\Theta}{dz^2} + 2\frac{db}{dz} + \Theta, \\ \frac{db}{dt'} &= \frac{d^2b}{dz^2} - \frac{d\Theta}{dz}, \end{aligned} \quad (80)$$

where we have introduced the dimensionless variables and parameters

$$\begin{aligned} \Theta &= \frac{T}{T_c - T_0}, \quad b = \frac{B}{B_e}, \quad z = \frac{x}{l}, \quad t' = \frac{t}{t_0}, \\ l &= \mu_0 \rho \frac{j_c B_e}{\nu}, \quad t_0 = \mu_0 \rho \frac{j_c^2 B_e^2}{\nu^2}. \end{aligned}$$

We present the small thermal and electromagnetic perturbations in the form

$$\begin{aligned} \Theta(z, \tau) &= \Theta \exp[\gamma t/t_0 + ik\xi + iq\zeta], \\ \epsilon(z, \tau) &= \epsilon \exp[\gamma t/t_0 + ik\xi + iq\zeta], \end{aligned} \quad (81)$$

where γ represents the eigenvalue of the problem to be determined and having wave numbers $k, q = 2\pi d/L$ in the $\xi = x/L$ and $\zeta = y/L$ directions, respectively. Solving the system equations (80) by using the solution (81) we obtain the following equation for the eigenvalues

$$\gamma^2 + [(1+\tau)(k^2 + q^2) - 1]\gamma + [\tau(k^2 + q^2) - 1](k^2 + q^2) - 2(k+q)^2 = 0$$

where τ is the ratio between the characteristic time of magnetic flux diffusion and the characteristic time of heat flux diffusion [4]. The instability criterion for flux jumping is determined by a positive values of the growth rate $\text{Re } \gamma > 0$. Let us first consider a simplest case, when $\tau=0$. Then, from the last relation we obtain

$$\gamma^2 + [(k^2 + q^2) - 1]\gamma - (k^2 + q^2) - 2(k+q)^2 = 0. \quad (82)$$

First, we notice that for perturbation uniform in x-direction $k=0$ the growth rate is positive $\text{Re } \gamma > 0$ for wave number $q < 1$. In such case the small perturbations grow with the maximal possible rate $\text{Re } \gamma = 1$. For the case $q > 1$, the growth rate γ is negative, consequently, the small perturbations always decay. Similarly, for the perturbations uniform in y-direction $q=0$, the growth rate is positive $\text{Re } \gamma$ only, if wave number is satisfied $k < 1$. As the wave number q approaches infinity $q \rightarrow \infty$, the growth rate approaches $\gamma = 1$ for $k = 0$ and small perturbations grow with time. It can be shown that, for the critical values of the wave number $k = k_c$, the growth rate is zero $\text{Re } \gamma = 0$. This instability occurs at $k < k_c$, and its criterion can be written as

$$k < k_c = \frac{1}{\sqrt{\tau}}.$$

The growth rate γ dependence on the wave number q for different values of k are demonstrated in Figs. (5a-5d) at $\tau = 0.1$. For high enough values of wave number k the system is stable. As the wave number k decreases, the growth rate γ increases. The branching instability will gradually appears for relatively small values of the wave number $k=0.5$.

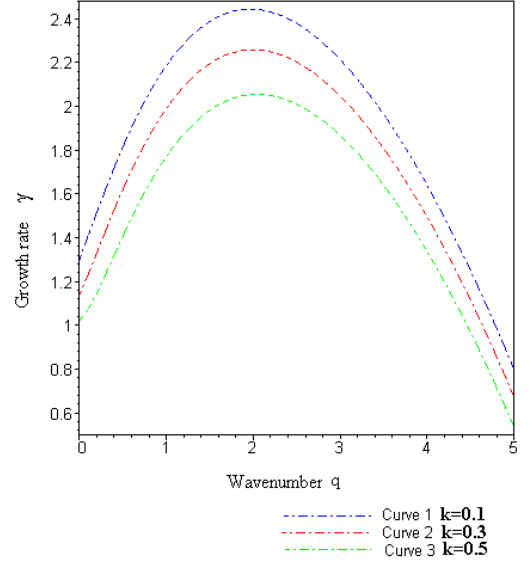
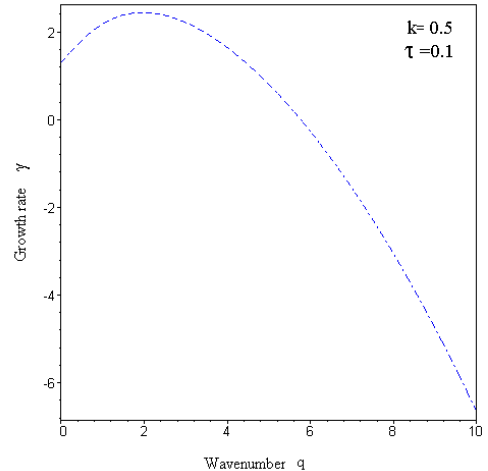


Fig.5a. The dependence of growth rate of the wave number $k=0.5, 0.3$ and 0.1 for $\tau = 0.1$.

Thus, on the basis of a linear analysis of a set of differential equations describing small perturbations of temperature and electromagnetic field we found that under some conditions a branching instability may occur in the sample.



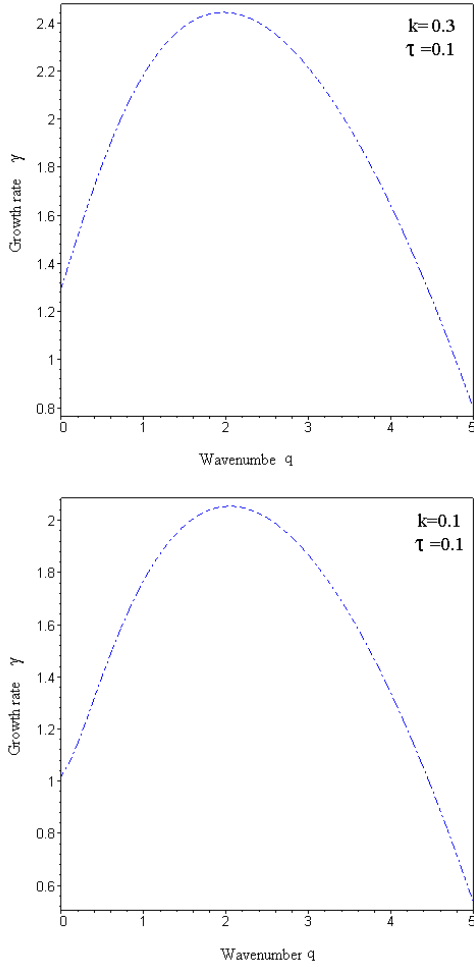


Fig.5b-5d. The dependence of the growth rate on the wave number for $k=0.5, 0.3$ and 0.1 for $\tau = 0.1$.

§2.2. Flux creep

Let us now study qualitatively, the problem of occurrence of the branching instabilities within the framework of flux creep problem with a nonlinear voltage-current characteristics. We assume that an applied field parallel to the surface of the sample. As we have showed above, for the flux creep problem the differential conductivity σ is determined by the following expression

$$\sigma = \frac{dj}{dE} = \frac{j_c}{nE_b} \quad (83)$$

Taking into account this flux creep relation, we write the system of differential equations, governing the small perturbations of the temperature and electromagnetic field in the form

$$\nu\gamma\Theta = \kappa \frac{d^2\Theta}{dx^2} + j_c\epsilon, \quad (84)$$

$$\frac{d^2\epsilon}{dx^2} = \mu_0\gamma \left[\frac{j_c}{nE_b}\epsilon - \frac{j_c}{T_c - T_0}\Theta \right]. \quad (85)$$

Next, we shall present a solution of these differential equations for $\Theta(x, t)$ and electromagnetic field $\epsilon(x, t)$ perturbations in the

following form

$$\Theta(x, t) = T_0(x) + (T_c - T_0)\Theta \exp[\gamma t/t_0 + iqz], \quad (86)$$

$$\epsilon(x, t) = E_b(x) + E_b\epsilon \exp[\gamma t/t_0 + iqz].$$

where $T_0(x)$ and $E_b(x)$ are solutions to the unperturbed equations obtained in the quasi-stationary approximation describing the background distributions of temperature and electric field in the sample. From solutions (86), one can see that the characteristic time of thermal and electromagnetic perturbations t is of the order of t_0/γ . Here, we have introduced the following dimensionless parameters and variables

$$t_0 = \frac{\sigma\nu a}{j_c}, \quad z = \frac{x}{l}, \quad l = \frac{\nu a}{\mu_0 j_c}, \quad q = \frac{\pi}{2} \frac{l}{L}.$$

As we mentioned above, the background temperature $T_0(x)$ is practically uniform over the cross-section of the sample and under this approximation we ignore its coordinate dependence. It turns out that these simplifications have no qualitative influence on the results but make it possible to perform analytical calculations completely.

Substituting the last expression (86) into the system equations (84), (85) one can get the following linearized system equations for Θ and ϵ

$$\tau q^2\Theta + \gamma\Theta + \frac{1}{n}\Theta - 2\left(\frac{1}{n}\right)^2\epsilon = 0, \quad (87)$$

$$q^2\epsilon + \gamma[\epsilon - n\Theta] = 0,$$

Solving the last system equations we obtain the following dispersion relation for the eigenvalue problem

$$\gamma^2 + \left[(1 + \tau)q^2 - \frac{1}{n} \right] \gamma + \left[\tau q^2 + \frac{1}{n} \right] q^2 = 0 \quad (88)$$

The instability of the flux front is defined by the positive value of the rate increase $\text{Re } \gamma > 0$. It can be seen that there is a critical cutoff wave number,

$$q_c = \frac{1}{\sqrt{\tau}}. \quad (89)$$

below which the system is always unstable at $n=1$. This instability appears first at $q=0$. In this case the small perturbations grow with the maximal possible rate $\gamma = 1$. The growth rate dependencies on the wave number for different values of τ are demonstrated in Figs. 6a-6c at $n = 1$. For high enough values of τ the system is stable. As the τ decreases, the growth rate γ increases. The branching instability will gradually appears for relatively small values of $\tau=0.5$.

According to inequality (89), the branching instability occurs at the threshold electric field $E = E_c$, which can be written as

$$E_c = \frac{\pi^2 \kappa (T_c - T_0)}{4 n j_c L^2}.$$

Taking into account that, the penetration depth L , the threshold field can be written at $B = B_{th}$ as

$$B_{th} = \frac{\pi}{2} \sqrt{\frac{\kappa (T_c - T_0) j_c}{n E_b}}.$$

The threshold field for branching instability, as can be seen from the last expression is highly sensitive to the critical current density and the shape of the background electric field E_b , generated by the varying of magnetic field. The threshold field B_j decreases

monotonously with increasing the background electric field E_b . If we assume that the background electric field E_b generated by a varying of magnetic field as $E_b \simeq \dot{B}_e$, for the considered simple geometry, then we can easily obtain the expression for the sweep rate dependence of the threshold field of branching instability.

Let us assume that the thermal diffusion is slower than the magnetic diffusion $\tau \ll 1$. In this limiting case, the instability criterion is determined as $q = q_c = 1$ for $n=1$, so the threshold field can be presented as

$$B_{th} = \frac{\pi}{2} \sqrt{\frac{\nu}{\mu_0} (T_c - T_0)}.$$

This is a well known adiabatic criteria [2], which assumes that the heat transport from the sample surface to the environment can be neglected.

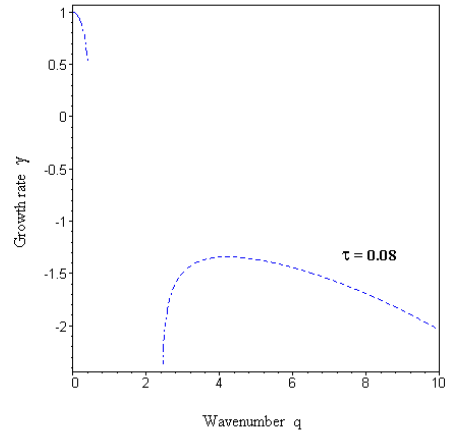
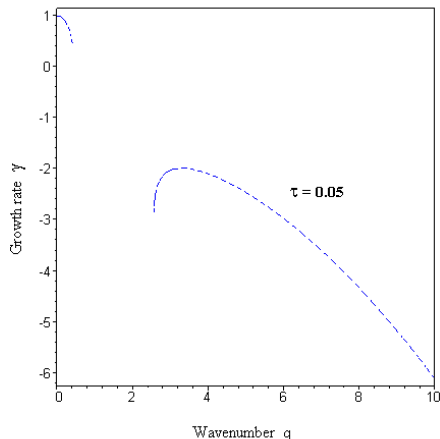
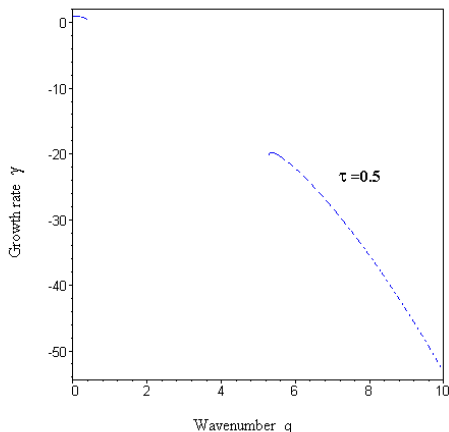


Fig.6a-6c. The dependence of the growth rate on the wave number for $\tau = 0.5, 0.05, 0.08$.

Fingering-like patterns were found theoretically recently by Rakhmanov et al. [90] on the linear analysis of a set of thermal and Maxwell equations for small temperature and electric field perturbations within the framework of adiabatic approximation. They calculated the stability criterion and estimated the build-up time and finger width. The fingering instability occurs at larger electric fields $E \geq E_c$, only. The authors believed that such fingering instability may develop to dendritic flux penetration into the sample. By solving the Maxwell and the thermal diffusion equations, it was shown that for small fields there are no solutions for perturbations growing in time, implying a stable situation. As the field increases the distribution can become unstable, with a fastest growing perturbation having a non-zero wave vector along the film edge. This means an instability will develop in the form of narrow fingers perpendicular to the edge – a scenario closely resembling the observed dendritic flux behavior.

§3. Dynamically driven flux instabilities

Recently, a many small in magnitude - mesoscopic in nature flux jumps has been observed in magnetization measurements of conventional and high- T_c superconductors at very low temperatures. It is interesting that the appearance of such type flux jumps can not be described in the framework of the traditional model of magnetothermal instabilities [1-9]. The main features of observed flux avalanches are the following: the first flux jump occurs at a values of the applied field much higher than full penetration field B_p ; the observed avalanches of almost the same amplitude look quite regular, they are essentially magnetic history sensitive; the avalanches exist only above threshold field of several tesla in magnitude as opposed to the low-field limit; its onset is independent on the sweep rate of the external magnetic field, a distinct contrast to flux jumps originating in a thermal instability in type-II superconductors; the avalanche size distribution is strongly peaked with a characteristic size, clearly distinct from the broad power-laws in the self-organized criticality concept; the jumps occur at significantly different fields on the increasing and decreasing branches of the hysteresis loop. Thus, it can be concluded that the onset of macroscopic flux jumps

in these experiments may be driven by a dynamic instability, which may be explained by means of a concept of self-organized criticality.

For example, Seidler et al. [95] argued for a dynamical origin of small vortex avalanches observed in their magnetization experiments and proposed an explanation based on self-organized criticality (SOC) [96, 97]. A new type of macroscopic flux jump with a narrow size distribution was observed by Zieve et al. [98] in untwined single crystals at very low temperatures (well below $T \sim 1\text{K}$), one not triggered by thermal instabilities. Interestingly, the avalanches exist only above threshold field and its onset is independent on the sweep rate. These avalanches occur at significantly different fields on the increasing and decreasing branches of the hysteresis loop. The authors concluded that the flux jumps in their experiments may be driven by a dynamic instability, which may be explained by means of a concept of self-organized criticality. Based on MD simulations Olson et al. [99] have showed that the dynamical instabilities are triggered when the external magnetic field is increased slightly, and are thus driven by a flux gradient rather than by thermal effects. The existence of SOC type of behavior flux avalanches recently has been experimentally observed and numerically adopted by many researchers [100-109]. Altshuler et al. [109] recently have analyzed in detail an experimental results on the flux avalanches which may be qualitatively understood by the concept of a self-organized criticality.

Huge "catastrophic", flux-jump-like avalanches associated with sudden movement of many vortices were observed by Behina et al. [110] in a superconducting Nb thick film during a slow sweep of external magnetic field ($\dot{B}_e \sim 1.1 \text{ Oe/s}$) by means a Hall probes. The obtained in a series of measurements avalanche size statistics indicated that the size distribution of these avalanches presents a power-law behavior only a limited range - in the small event region. The authors believed that in contrast, at low temperatures and fields, huge avalanches which may be related to thermal instability of the Bean state dominate the dynamic response of the sample.

Irregular and non-periodic flux jumps were observed by Majumdar et al. [111] in the low field magnetization measurements at different field sweep rates in the heavy fermion superconductor samples. The large in magnitude flux jumps were observed at the highest sweep rates. The magnitude of these jumps decreases slowly with decreasing of temperature below 1.7 K and the jumps are completely absent at 1.5 K. They argued that the observed flux jumps are due to local flux entry through the surface or geometrical barriers. The asymmetry of the flux jumps with respect to increasing and decreasing part of the magnetization loop clearly indicate the existence of barriers at surface of the sample.

Flux jumps that differ qualitatively from well-known magnetothermal instabilities have been observed by Milner [112] and Gerber and Milner [113] in thin single crystals of high- T_c superconductors in the fields up to 17 T at the temperatures down to 0.3 K, using magnetometric, calorimetric and induction pick-up techniques. The flux jumps start above full penetration field B_p , demonstrating clear periodicity in the slowly changing magnetic field. The magnetization hysteresis loop is non-homogeneous, consisting of high steps, which reflect the global redistribution of the magnetic flux in the sample. It was found that the frequency of flux jumps is strongly temperature dependent. Milner

proposed a few variants to explain about the origin of the low-temperature/high-field magnetization jumps observed in their experiments. Using a Hall probe sensor Terentiev et al. [114] have observed a quasi-periodic flux instabilities below a certain temperature ($T \sim 3 \text{ K}$) in a superconducting Nb thin films by a square lattice of Ni dots. The magnetization measurements indicated that the Ni dot lattice exerts a crucial influence on the appearance and nature of the instabilities. On the analysis of magnetization curves the authors have found that the quasi-periodic instabilities as unexpected low-temperature matching anomalies, most probably initiated near the film edge, where flux density is much lower than in the film interior.

§4. Flux avalanches

Recently, Chabanenko et al. [26] have reported an interesting phenomenon in their experiments - convergent oscillations of the magnetic flux arising from flux jump avalanches. The authors argued that the observed oscillations due to flux avalanches can be interpreted as a result of the existence of a definite value of the effective vortex mass [27]. Thus, it is necessary to take into account collective modes, i.e., the inertial properties of the vortices in studying the dynamics of the flux avalanches. Prior to the jump, the mixed state of superconductors is characterized by nonuniformly distributed magnetic induction localized near the surface. As a result of the avalanche, the flux rushes from either sides of the sample towards the center [26]. Two fronts of the penetrating flux collide in the center of the sample and, owing to the existing vortex mass, give rise to the local surplus density of the magnetic flux that exceeds the value of the external magnetic field. The repulsion force in the vortex structure at the center of the sample that have resulted from its compaction, initiates the wave of the vortex density of the inverse direction of propagation. Upon reaching the surface, this wave is reflected from it. This results in the oscillations in the vortex system [26]. The limitation of the number of oscillations observed is caused by the existence of damping. One succeeds in observing the oscillation of the vortex density only owing to a strong compression of the vortex structure as a result of the giant avalanche-flux [17, 24-26].

In this section, we study the dynamics of the magnetic flux avalanches, which take account inertial properties of the vortex matter.

In the flux flow regime the electric field $\vec{E}(r, t)$ induced by the moving vortices is described

$$\vec{E} = \vec{v}\vec{B}. \quad (90)$$

To obtain quantitative estimates, we use a classical equation of motion of a vortex, which it can derived by integrating over the microscopic degrees of freedom, leaving only macroscopic forces [32]. Thus, an equation of the vortex motion under the action of the Lorentz, pinning, and viscosity forces can be presented as

$$m \frac{dV}{dt} + \eta V + F_L + F_p = 0. \quad (91)$$

Here m is the vortex mass per unit length, $\vec{F}_L = \frac{1}{c} \vec{j} \vec{\Phi}_0$ is the Lorentz force, $\vec{F}_p = \frac{1}{c} \vec{j}_c \vec{\Phi}_0$, η is the flux flow viscosity coefficient [32]. For simplicity we have neglected the Magnus force, assuming that it is much smaller than the viscous force (for example,

for Nb see, [26]). In the absence of external currents and fields, the Lorentz force results from currents associated with vortices trapped in the sample.

In combining the relation (90) with Maxwell's equation (2), we obtain a nonlinear diffusion equation for the magnetic flux induction $\vec{B}(r, t)$ in the following form

$$\frac{d\vec{B}}{dt} = \nabla(\vec{v}\vec{B}). \quad (92)$$

$$m\frac{dV}{dt} + \eta V = -\frac{1}{c}\Phi_0(j - j_c), \quad (93)$$

The temperature distribution in superconductor is governed by the heat conduction diffusion equation

$$\nu(T)\frac{dT}{dt} = \nabla[\kappa(T)\nabla T] + \vec{j}\vec{E}, \quad (94)$$

Let us present a solution of equations (90-94) in the form

$$\begin{aligned} T &= T_0 + \Theta(x, t), \\ B &= B_e + b(x, t), \\ V &= V_0 + v(x, t) \end{aligned} \quad (95)$$

where $T_0(x)$, $B_e(x)$ and $V_0(x)$ are solutions to the unperturbed equations, which can be obtained within a quasi-stationary approximation. Substituting the above solution (95) into equations (92-94) we obtain the following system of differential equations [26]

$$\frac{d\Theta}{dt} = 2v - \beta\Theta, \quad (96)$$

$$\mu\frac{dv}{dt} + v = -\frac{db}{dx} + \beta\Theta, \quad (97)$$

$$\frac{db}{dt} = \left(\frac{db}{dx} + b\right) + \left(\frac{dv}{dx} + v\right), \quad (98)$$

where we have introduced the dimensionless variables

$$b = \frac{B}{B_e} = \frac{B}{\mu_0 j_c L}, \quad \Theta = \frac{\nu\mu_0}{B_e^2}, \quad v = V\frac{t_0}{L}.$$

$$z = \frac{x}{L}, \quad \tau = \frac{t}{t_0} = \frac{\Phi_0}{\eta} \frac{B_e}{\mu_0 j_c L^2} t,$$

and parameters

$$\mu = \frac{\Phi_0}{\mu_0 \eta^2} \frac{B_e}{2L^2}, \quad \beta = \frac{\mu_0 j_c^2 L^2}{\nu(T_c - T_0)}.$$

Assuming that the small thermal and magnetic perturbations has form $\Theta(x, t), b(x, t), v(x, t) \sim \exp[\gamma t]$, where γ is the eigenvalue of the problem to be determined, we obtained from the system Eqs. (96)-(98) the following dispersion relations to determine the eigenvalue problem

$$\begin{aligned} (\gamma + \beta)\frac{d^2 b}{dx^2} - [(\gamma + \beta)\mu - 2\beta]\frac{db}{dx} + [(\mu + 1)\gamma^2 + \\ + [(\mu - 1)\beta - \mu - 1]\gamma - (\mu - 1)\beta]b = 0 \end{aligned} \quad (99)$$

An analysis of the dispersion relation shows that, the grows rate is positive $\text{Re } \gamma > 0$, if $\mu > \mu_c = 2$ and any small perturbations will grow with time. For the case when $\mu < \mu_c$, the growth rate is negative and the small perturbations will decay. At the critical value of $\mu = \mu_c$, the growth rate is zero $\gamma = 0$. For the specific

case, where $\mu = 1$ the growth rate is determined by a stability parameter β . Thus, the stability criterion can be written as

$$\beta > 1. \quad (100)$$

For the case, where thermal effects is negligible ($\beta = 1$) we may obtain the following dispersion relation

$$\frac{d^2 b}{dx^2} - \mu\frac{db}{dx} + (\gamma - 1)(\mu + 1)b = 0. \quad (101)$$

Seeking for $b \sim \exp(ikx)$ in dispersion relation, the growth rate γ dependence can be obtained as a functions of wave number k .

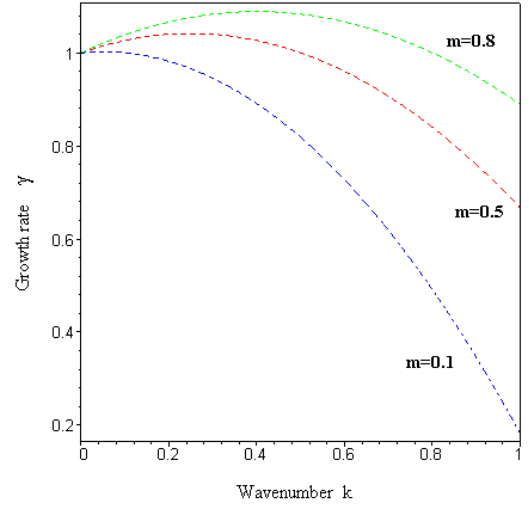


Fig.7a. The dependence of the growth rate on the wave number for $\mu = 0.1, 0.5, 0.8$.

The stability of the system depends on the growth rate, γ , given in (101). We analyze the growth rate of small perturbations as a function of wave number k . When $k < k_c = \mu$ the growth rate is positive and any small perturbations will grow with time. For wave number $k > k_c$, the growth rate γ is negative. Consequently, the small perturbations always decay. It can be shown that, for wave number $k = k_c$ the growth rate is zero $\gamma = 0$. As the wave number approaches zero $k \rightarrow 0$ or infinity $k \rightarrow \infty$ the growth rate approaches $\gamma = 1$ and small perturbations grow with time. As the wave number approaches unity $k = 1$ the growth rate is determined by the value of μ

$$\gamma = \frac{2\mu}{\mu + 1}.$$

For $\mu = 0$ the growth rate is zero $\gamma = 0$. For $\mu = 1$ the growth rate is unity $\gamma = 1$. Since the growth rate is zero at the critical wave number and approaches to unity in the limit of zero wave number, there must exist a wave number in between that maximizes the growth rate. Figs. (7a-7d) show the growing rate, γ , as a function of the wave number k , for different values of the parameter μ . As the value of μ increases, the corresponding growth rate increases.

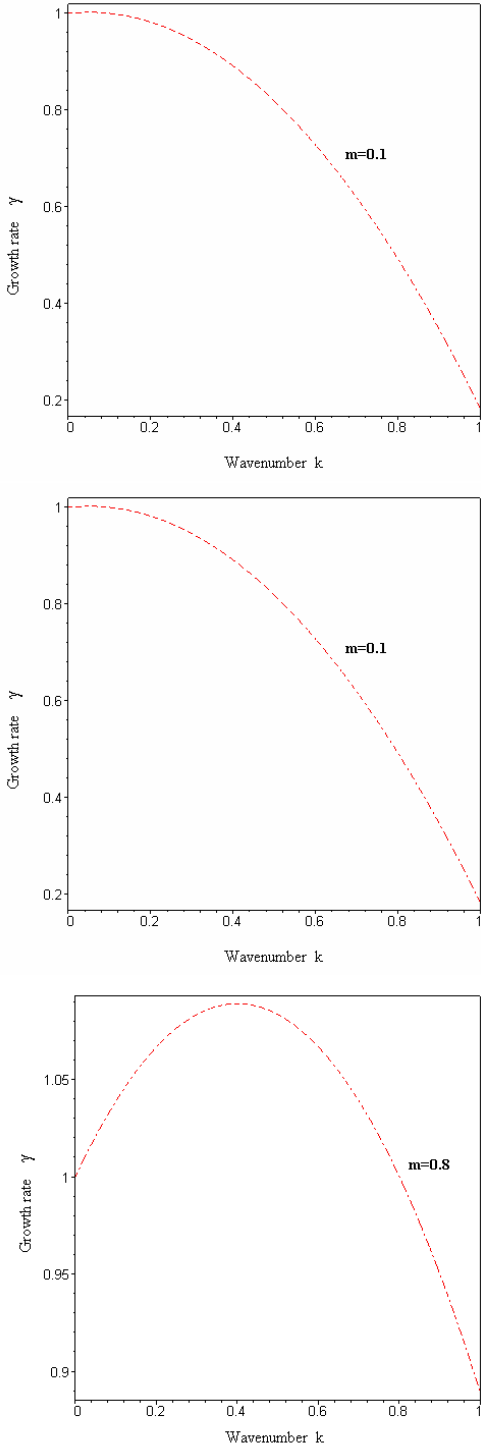


Fig.7b-7d. The dependence of the growth rate on the wave number for $\mu = 0.1, 0.5, 0.8$.

Thus, we show that at under some conditions flux jump avalanches may occur in superconductor sample, which take into account inertial properties of the vortices.

§5. Second magnetization peak

The second-peak effect in the magnetization curve is one of the most remarkable features in the vortex state of both low and high- T_c superconductors. The second magnetization peak (or "fishtail") as a function of applied field was observed in a low-temperature superconductor materials [115-118] and high-temperature superconductors [119-130]. The second peak is expected to give an important clue in the understanding of the complex vortex-matter phase diagram in low and high- T_c superconductors. In addition, different interpretations for the second peak have been discussed in literature, however, the mechanism of the second peak remains unclear. These range from the enhancement in pinning due to matching effects in oxygen deficient structures [119], the collective creep phenomenon [120, 130], matching effect [131, 132], the dimensional crossover [133], the surface barrier effect [134], the thermomagnetic instability [135-139], elastic to plastic creep [122-124], crossover in the pinning regimes, e.g. from single-vortex pinning to a pinning of vortex bundles [121]. Many theoretical and experimental publications dealing with the second magnetization peak effect have been recently published, the interpretation of this effect is still rather controversial. No single mechanism exist until day, which may explain the nature of these effects that were observed in a large amount of superconducting samples.

§5.1. Thermomagnetic instability

For low- T_c superconductors (Nb), the second magnetization peak occurs at lower temperature region during the magnetic flux penetration, but at higher values magnetic fields close to the upper critical field H_{c2} . Recent experimental investigations indicated that second magnetization peak is probably originated by a thermomagnetic instabilities that occur in the low-temperature region, far below H_{c2} [135-139]. In particular, such flux-jump instabilities in Nb thin films have been studied by Esquinazi et al. [136] on the basis of isothermal and global magnetization measurements as a function of applied field with a SQUID and μ -Hall sensors, respectively. Large jumps as well as pronounced irregularities of large scale gradients in the vortex density has been observed at low temperature region ($T \sim 3$ K) and at low applied fields ($H \sim 100$ Oe) in the magnetization $M(H)$ curve. The existence of the second magnetization peak in a thick Nb film, which was clearly produced by magneto-thermal instabilities recently have been reported by Kopelevich et al. [137, 139] using a SQUID and Hall array measurements. The magnetization peak appears at fields higher than the first maximum observed usually in a zero-field-cooled state, but much lower than the upper critical magnetic field H_{c2} . The flux jumps were clearly observed up to the second magnetization peak at $B_{sp} \approx 1300$ Oe. The first flux jump field B_{fj} was discussed and numerically estimated in this work. This estimation shows that the first peak $H_{fp} \sim 100$ Oe observed in the magnetization curves is of the order of the first flux jump field B_{fj} . Additionally, the temperature and sample size dependencies on the magnetization jumps were investigated. It has been shown that the maximum dissipated magnetic energy during the flux jump process - the maximum

temperature at the first flux jump may increase substantially at $B \geq B_{fj}$ due to the decrease of the specific heat and the increase in the critical current density in the sample. Thus, under certain experimental conditions, which depend on the thermal and magnetic diffusivities and the thermal coupling of the sample with its environment, this temperature change can produce flux jumps instabilities. It was also shown [136] that the field of the second peak increases with the thickness and/or width of the film as expected for measurements in transverse geometry. The jumps become smaller in magnitude or even vanish with a reduction of the film thickness. The authors have pointed out that careful characterization of the second peak in Nb films is important and may contribute to understand the anomalous behavior of the magnetization curve $M(H)$ measured in high- T_c as well as conventional superconductors which in some cases is interpreted in terms of a vortex lattice phase transition [136]. Similar magnetization measurements on the second magnetization peak were performed recently Stamopoulos et al. [140] at different magnetic field sweep rates in superconductor thin films. Thermomagnetic flux jump instability was observed at temperature $T=7.2$ K. The magnitude of the first flux jump field B_{fj} coincides with the first peak B_{pj} at a characteristic temperature $T = 7.2$ K. The first flux jump field remains constant B_{fj} Oe at low temperature region $T < 6.4$ K. The dependence of the first flux jump field on sweep rate of the magnetic field has been studied, also. Surprisingly that the observed first flux jump field is not inversely proportional to the sweep rate of the applied field, which in contrast to theoretical concepts for the flux jumping and other experimental dates [8, 15, 136, 17].

Let us qualitatively estimate the temperature dependence of the first flux jump field $B_{fj}(T)$, which occurs at low temperature part of the magnetization curve. According to conclusion of Ref. [136] the first magnetization peak $B_{fp}(T)$, which is nearly independent of the sweep rate is of the order of the field at which the first jump $B_{fj}(T)$ occurs. It is reasonable then that the temperature dependence of the first flux jump field $B_{fj}(T)$ can be fit according to the adiabatic critical state theory

$$B_{fj} = \sqrt{\pi^3 \frac{\nu j_c}{-dj_c/dT}}.$$

In order to compare the last formula with experimentally determined first flux jump field, one must know the temperature dependencies of the critical current density and the specific heat of the sample. As has been mentioned in literature [136] a quantitative estimation of $j_c(T)$ from the available experimental and theoretical models is difficult because of the uncertainty in the values of the critical current j_c at a given field and temperature. To determine $j_c(T)$, different approaches have been taken. Empirically, the critical current density $j_c(T)$ can be presented in the form

$$j_c = j_0 [1 - t^n]^m. \quad (102)$$

where $1 < m < 2$. The different exponents $n=1$ and 2 refer to the most common cases discussed in the literature, where the critical current exhibits a linear and a quadratic dependence on $t = T/T_c$.

There is experimental evidence [41, 33], which indicates that the temperature dependence of the critical current density approximately linear at low temperatures ($n=m=1$). On the other

hand, at temperatures well below T_c the magnitude of the specific heat decreases rapidly with decreasing temperature, so we can estimate the specific heat as $\nu \simeq (T/T_c)^3$. Using the above values of temperature dependencies of the specific heat and the critical current density we obtain the following stability criterion [1, 2]

$$B_{fj} = T_c^2 \sqrt{\pi^3 T^3 (T_c - T)}.$$

Combining all these equations, one obtains a theoretical $B_{fj}(T)$ curve as shown in Fig. 3. Thus, it can be concluded that the temperature dependence of the first penetration field $B_{fp}(T)$ is consistent with the temperature dependence of the first flux jump field $B_{fj}(T)$, as demonstrated in figure 8.

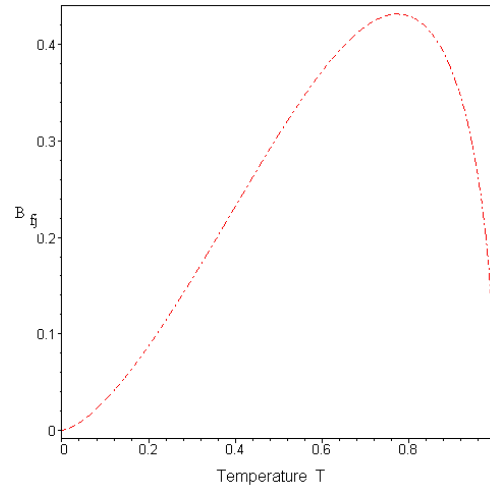


Fig.8. The temperature dependence of the first flux jump field

The dome-like profile of the temperature dependence of the first flux jump field at low fields and temperatures have been observed in many experiments [136, 143]. Thus, our analysis shows that the temperature dependence of the first flux jump field $B_{fj}(T)$ is consistent with the model which ascribes the first peak (onset field) of the second magnetization peak. This scenario is consistent with the observation of a crossover in the field profiles across the sample, from profiles characteristic of geometrical barrier with weak pinning at fields below the B_{fp} , to Bean-like profiles at fields above the first peak. The results of experiments, obtained by Esquinazi [136] have shown that near the first flux jump field the vortices penetrate the sample, forming a droplet with a dome shape far away from the Nb film edges, i.e., near the center or at the center of the sample, depending on the temperature. A further increase of the external field does not change homogeneously the flux profile inside the sample, but part of the vortices remain pinned. The domelike flux profiles at low enough fields have been also observed in high-temperature platelet-shaped samples (see, for example [143] due to the existence of a geometrical or edge barrier given by the shape of the sample. It has been claimed [136, 138] that the observed domelike shape of the field profile cannot be due to edge barrier. The observed strong temperature dependence of the flux profile at the first flux jump field $B_{fj}(T)$, speaks for the influence of a thermomagnetic instability [136]. After the first flux jump, the increase of field moves vortices from the edges and a Bean-like profile starts to develop. The higher the applied field, the lower

the critical current density and therefore the larger is the penetration of the Bean-like profile into the sample up to the second magnetization peak field B_{sp} .

The results of [136] indicated that the temperature dependence of the second peak field $B_{sp}(T)$ has shown a similar temperature dependence as the upper critical field $H_{c2}(T)$. So, at high enough fields and temperatures the temperature dependence of second magnetization peak field can be well fitted by

$$B_{sp}(T) = B_0 (1 - t^2).$$

where B_0 is a constant parameter. The temperature dependence of the field $B_{sp}(T)$ is shown in Fig.9.

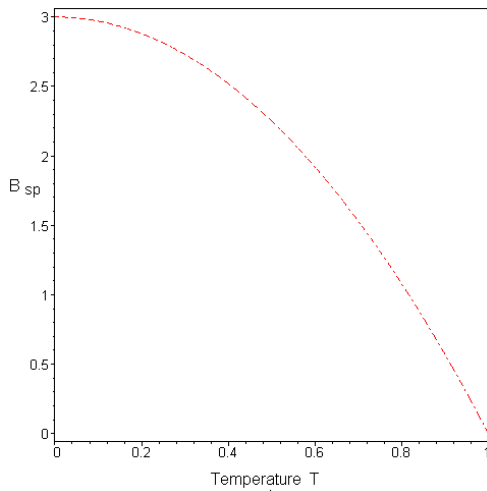


Fig.9. The temperature dependence of the second magnetization peak.

As can be seen it reflects, roughly the temperature dependence of the upper critical field. At higher temperatures and fields (near the upper critical field), where the second magnetization peak appears the temperature dependence of the critical current density can be presented as

$$j_c(T) = j_c(0) (1 - t^2)^2.$$

commonly accepted in literature [33] ($n=m=2$). Assuming that the thermal conductivity is a linear function of temperature, we can easily obtain an expression for the temperature dependence of the field $B_j(T)$

$$B_j(T) \approx B_{10} \sqrt{t(1-t)^2}.$$

where B_{10} is the free parameter.

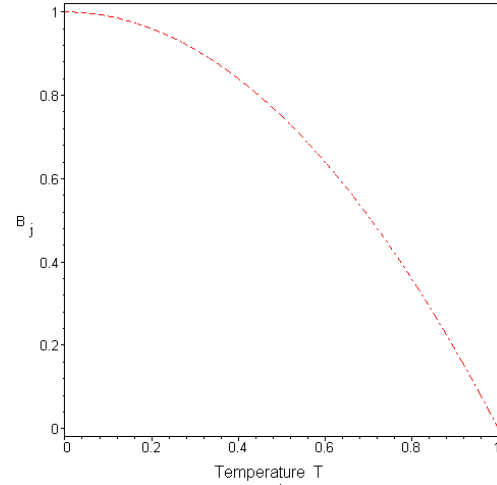


Fig.10. The temperature dependence of the threshold field $B_j(T)$.

It should be noted that the stability criterion (43) strongly depends on the sample geometry. For the case of infinite slab geometry or long cylindrical sample with an external magnetic field applied parallel to its surface or axis the role of dimension is played by the sample diameter $d = 2l$. Then the critical dimension of the sample is determined from the relation

$$B_j = \frac{4\pi}{c} j_c d_c,$$

Then for the sample with a dimension d smaller than the critical one $d < d_c$, no flux jumps occur at any temperature for any external magnetic field. Thus by reducing the sample dimension it is possible to avoid flux jumps. In the case of disc geometry the stability criterion can be modified as

$$\beta = \frac{\pi j_c^2 r d}{\nu(T_c - T_0)}, \quad (103)$$

where r is the radius and d is the diameter of the disc. In this case the experimental value of stability parameter for Nb disc samples approximately is equal to $\beta=1.2$ for the typical values of parameters j_c , ν and r, d at helium temperature. For thin films in an external magnetic field perpendicular to their surface, the role of the critical dimension from the point of view of occurrence of flux jumps is played by their thickness. The result obtained for bulk sample may be modified for thin samples in a perpendicular field multiplying by a numerical factor. The dependence of the maximum in the width of the magnetization hysteresis loop and transition field B_j - on the sample geometry has been reported for Nb films and single crystals [137]. It was found that the second magnetization peak vanishes in both superconductors for small enough dimensions of the sample. According to flux jump theory the sample dimension is

$$d = \frac{c}{4\pi j_c} B_j.$$

This model predicts the vanishing of the second magnetization peak with decreasing the sample size. The estimation of the critical thickness of the sample from the measured values of parameters and B_j show that the necessary requirement for the avoiding flux jumping the sample thickness has to be lower than

its critical value, of the order of $100 \mu m$ [136]. In agreement with this model, the second peak vanishes in thin film superconductors when the lateral sample size becomes d less than $d < d_c \simeq 100 \mu m$. For the transverse geometry of a rectangular thin film the effective size d of the sample above which flux jump occurs is [137]

$$d < d_c = \left[\frac{wl}{2} \right]^{1/2}.$$

where $d \ll l, w$; l is the length, w is the width of the film. For the numerical magnitudes of a typical parameters, the critical size d of the sample for the transverse geometry should be less $\leq 500 \mu m$ [137]. Hence, the authors argued that the existence of the second magnetization peak in thick Nb film can be should be clearly produced by thermomagnetic flux jump instabilities [8, 9]. The authors [136] believed a such sample size dependence of the threshold field as well as the observed dependence of the amplitude and number of flux jumps on the field sweeping rate \dot{B}_e provide the experimental evidence for the thermomagnetic origin of the second magnetization peak in Nb samples. Let us estimate the temperature dependence of the effective sample size d_c for a typical experimental values of parameters for Nb. In Fig. 11 we show the temperature dependence of the sample size d . Roughly, it increases linearly with temperature. This result was obtained from the relation for the stability criterion (43) and it can be considered as empirical that we assumed a linear dependence of the thermal conductivity $\kappa = \kappa_0(T/T_c)$, where κ_0 is the constant parameter, as suggested by low-temperature data for Nb and linear temperature dependence of the critical current density

$$d \approx \frac{\pi}{2} \sqrt{t(1-t)^{-1}}.$$

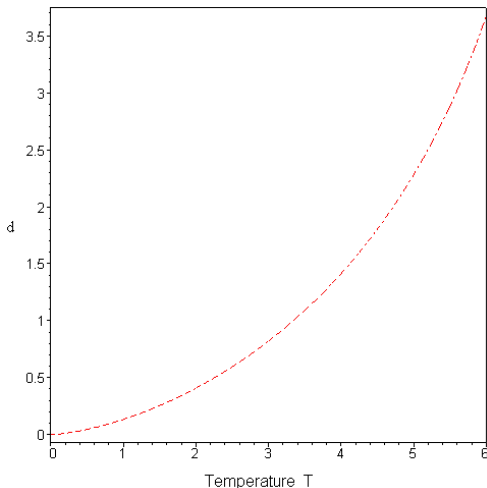


Fig.11. The temperature dependence of the effective sample size.

Nabialek et al. [17] have shown that due to the existence of a critical dimension the flux jump instability in high- T_c superconductors was observed only in relatively large single crystals. No flux jumps has been observed in ceramic materials, because the critical dimension in these materials is limited by the grain size, which is typically very small. Thus, the nature of origin and further development of the flux jump instabilities may be different in thin films and bulk samples [93]. In bulk samples flux

jump can be triggered when the gradient of magnetic flux profile inside the sample exceeds critical value B_j . In each jump many vortices are involved in the avalanche process, which normally expands to a large part of the sample volume. On the other hand, in bulk samples, there are many large grain boundaries, which act as strong pinning centers. The gradient of the flux profile near these boundaries can be broken at a certain limit. Once a blast occur, the thermal energy induced by drastic flux motion cannot easily diffuse out and be carried by the environment. Therefore this self-heating will lead to an increase of temperature in the region in which the flux instability occurs, leading to a large jump on the magnetization. One can understand from this picture that the number of flux jumps cannot be large in bulk samples. Such instabilities in the bulk superconductor samples can be qualitatively understood based on the adiabatic theory [1]. In thin films, the situation is completely different and the observed small and irregular avalanches cannot be explained by the adiabatic theory. There are generally more defects or pinning centers in thin films may be observed a small avalanches. Due to the high density of small defects formed during the preparation process there are many places for the avalanche to occur in thin films. Thermal diffusion is much easier in thin films due to their very small thickness and large surface area exposed to the environment. Therefore in thin films each avalanche is small in magnitude but the number of avalanches can be huge. This picture may give an explanation to many small vortex avalanches observed in thin films. Since maintaining good thermal contact throughout a sample is more difficult for bulk samples than for thin films, thermally driven avalanches should occur more easily as sample thickness increases [93].

We have studied the second magnetization peak in the framework of a thermomagnetic model and demonstrated by a qualitative agreement of the theory with experimental results [135-139]. In other words, our theoretical analysis on flux jump instability qualitatively reproduces experimentally observed in [135-139] second peak features: the sample size dependence of the threshold field, the temperature and sweep rate dependencies of the first flux jump field and etc.,

Magnetic flux jump instabilities have also been observed in high temperature superconducting materials [2, 18, 62, 19, 62, 17]. In the following we shall discuss some recent existing theoretical models, which may give a qualitative description on the nature of the second magnetization peak and its onset for superconducting materials. Both the onset field B_{on} and the second peak field B_{sp} exhibit strong temperature dependence up to the close vicinity of critical temperature T_c . To understand the origin and nature of the onset of second peak it is very useful to study the temperature dependence of the field B_{on} . Let us study the temperature dependence of the onset field within the framework above mentioned theoretical models. In the last decade, many different by each other hypotheses have been proposed to explain the nature of the second peak effect. For example, Krusin-Elbaum et al. [121] ascribe the occurrence of the peak effect to the crossover between two collective vortex creep regimes; from single to collective vortex creep regime. The independence of the magnetic moment from the applied field for low temperature isothermal loops is interpreted by them as the single vortex creep regime [121]. The authors believed that the peak effect is not likely to be observed on very short time scales due to the fact that the relaxation is much faster in the single

vortex creep regime than in the collective vortex creep regime. Yeshurun et al. [130] also assigned dynamical characteristics to the appearance of the peak effect. In other studies, the influence of oxygen content on the peak behavior is discussed [142]. Zhukov et al. [142] found that the peak effect was present at high temperatures for all oxygen contents, however the peak's height takes the smallest value for the state closest to stoichiometric status, which means that oxygen deficiency is necessary for achieving greater pinning and therefore higher critical current density. In some cases a correlation between the peak effect and the oxygen concentration is found to be the source of peak effect. Daumeling et al. [119] argued that a field-induced pinning enhancement in oxygen-deficient regions may be the source of the second magnetization peak in superconductor sample. The authors proposed that oxygen-deficient areas had become normal as the field was increased, as a result of their lower T and H. These areas thus become new pinning centers. Therefore any change in oxygen content or distribution should lead to suppression or appearance of the peak effect. In a quite different model, the peak effect is considered as a result of the matching effect [132], where matching of the vortex lattice with the defect structure leads to pinning enhancement. However, the temperature-dependent nature of the peak strongly rules out the matching effect as the origin of the peak effect.

The experiments of magnetic relaxation are the most extensively used tools to study the vortex dynamics in a variety of superconducting materials [121-124]. The relaxation rate S as a function of H can provide relevant information about the pinning mechanism [121]. It has been demonstrated [121] that the relaxation rate drops as field increases from below B_{sv} up to a field close to second magnetization peak field B_{sp} , increasing again as H become larger than B_{sp} . Results of this magnetic relaxation experiments have shown the existence of a crossover in the pinning mechanism at B_{sv} , where apparently, this crossover occurs without a change in the behavior of the relaxation rate with field. The peak in S(H) has been recently interpreted [121] as a consequence of the crossover from individual to collective regime. At the high-temperature side of the peak in S(H), relaxation is anomalous in the sense that the relaxation rate varies non-monotonically with time. It has been shown [121] that the anomalous relaxation that occurs on the high-temperature side of the peak in S(H) indicates that the vortex structure undergoes a change in the relaxation regime. The second magnetization peak occurring at B_{sp} is formed by a crossover in the pinning mechanism, from collective to plastic pinning as the field increases [122]. Results of this work show that the temperature dependence of the second magnetization peak position, B_{sp} is well explained in terms of a plastic motion of the vortex lattice. An analysis of the relaxation data shows that the peak field is moving with time to lower values. The dynamic picture is also consistent with results by Yeshurun et al. [130], showing a clear time dependence of the second peak. Both studies show that the peak is virtually absent when the loops are measured on a short time scale while the peak gradually appears as the time scale is expanded. As pointed out in the previous section, the activation energy grows with B below the second peak and decreases after the peak. This crossover in the field dependence indicates an elastic-to-plastic creep crossover around the peak-field similar to that observed in other materials [122-130].

§5.2. Collective creep

One of simple situation to introduce the concept of weak collective pinning is an isolated vortex in an isotropic superconductor subject to pinning by randomly distributed point defects [141]. We shall study the problem within a continuum elastic description of the flux-line lattice, with a potential energy given by the combination of the elastic energy, the pinning energy and the action of the Lorentz force

$$E_e = c_{66}u^2L + e_1\frac{u^2}{L} - (\gamma\xi^2L)^{1/2}. \quad (104)$$

where u and L are the transverse and longitudinal sizes of vortex distortion respectively, $\gamma = f_p^2 n_i \xi$ is the disorder parameter; f_p is the elementary pinning force, n_i is the density of pinning centers, $c_{66} = e_0/4a_0^2$ is the vortex-lattice shear modulus; $e_1 = e^2 e_0$ is the vortex line tension, e is the anisotropy parameter, e_0 is related to the energy of a vortex line per unit length $e_0 = (\Phi_0/4\pi\lambda)^2$, $a_0 = \sqrt{\Phi_0/B}$ is the vortex line spacing, Φ_0 is the flux quantum, λ is the penetration depth, ξ is the coherence length. The characteristic longitudinal length L_0 , which determines the size of elastic screening of local distortions of the vortex line can be evaluated by minimizing of the elastic energy with respect to L

$$L_0 = \sqrt{\frac{e_1}{c_{66}}}.$$

The characteristic elastic energy of the vortex thus becomes

$$E_e = \frac{ee_0}{a_0}u^2. \quad (105)$$

The collective pinning length can be evaluated by balancing the elastic energy cost and the pinning energy gain associated with a small displacement of a region of linear size L

$$L_c = \left(\frac{e_0^2\xi^2}{\gamma}\right)^{1/3}. \quad (106)$$

Equating the resulting pinning force and the Lorentz force on segments of the length L_c allows one to obtain the critical current density for the case of weakly pinning point defects and small applied fields

$$j_{sv} = \frac{c}{\Phi_0} \left(\frac{\gamma}{L_c}\right)^2. \quad (107)$$

Let us estimate for the single-vortex—small-bundle crossover field B_{sv} , where the system changes from single-vortex creep to collective creep of small bundles. This crossover field B_{sv} is determined by the condition [49]

$$L_c = ea_0.$$

This condition is equivalent to

$$B_{sb} = \beta \frac{j_{sv}}{j_0} B_{c2}, \quad (108)$$

where $\beta \approx 5$ is the constant parameter, $j_0 = 4B_c/3\sqrt{6}\mu_0\lambda$ the depairing current density, $B_c = \Phi_0/2\sqrt{2}\pi\lambda\xi$ the thermodynamic critical field, $B_{c2} = \mu_0\Phi_0/2\pi\xi^2$ the upper critical field.

As can be seen from the last expression, the temperature dependence of the crossover magnetic field B_{sv} is determined by the

temperature dependence of the intrinsic superconducting parameters, such as the coherence length $\xi(T)$ and the magnetic penetration depth $\lambda(T)$, and the disorder parameter γ of the vortex system. According to G. Blatter et al. [49], defects can interact with the vortices in two different ways. They may cause a spatial variation of the transition temperature (δT_c -pinning) and a spatial modulation of the mean free path (δl -pinning). In both cases, the influence of disorder is described by a disorder parameter γ , proportional to the defect density and the temperature dependence of γ is different for the two cases. For δT_c -pinning, $\gamma = \lambda^{-4}$, while for δl -pinning, $\gamma = \lambda^{-4}$. Thus, depending on the type of pinning the crossover field can be either an ascending or descending function of temperature. Considering the functional form of the disorder parameter for δT_c -pinning, $\gamma = \lambda^{-4}$. Within the frame of the Ginzburg-Landau theory $\lambda(T) = (1 - t^4)^{-1/2}$ and $\xi(T) = [(1 - t^2)/(1 - t^2)]^{-1/2}$, where $\lambda(0)$ and $\xi(0)$ is the penetration depth and the coherence length at $T=0$ K. Inserting the values of the coherence length $\xi(T)$ and the penetration depth $\lambda(T)$ into the last equation for $B_{sp}(T)$ we obtain the following expression for the crossover field B_{sv} in the single creep regime for the case δT_c pinning

$$B_{sv} = B_{sv}(0) \left(\frac{1 - t^2}{1 + t^2} \right)^{2/3}, \quad (109)$$

and δl -pinning, respectively

$$B_{sv} = B_{sv}(0) \left(\frac{1 - t^2}{1 + t^2} \right)^2. \quad (110)$$

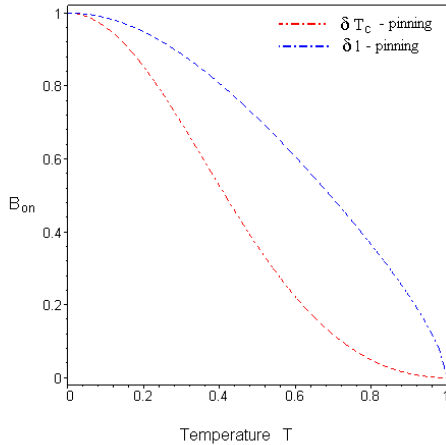


Fig.12. Crossover field as a function of temperature corresponding to δl and δT_c pinning.

The data in Figure 12 clearly show that only, the δT_c -pinning formula can explain the temperature dependence onset field B_{on} , accurately. Thus, a crossover from individually pinned regime to a collectively pinned regime is to be anticipated at a threshold field B_{sv} , above which vortex-vortex interactions become dominant. At low temperatures with the numerical values λ and ξ we find that B_{sv} is of the order of 1.7 T. This is justified in the limiting case of small magnetic fields. Consequently, the transverse correlation length of the flux lattice $L_c=1$ is approximately equal to $0.1a_0$, i.e. it is much lower than the intervortex spacing a_0 .

Thus, the vortex system is in the single-vortex pinning regime at low fields.

As we have already mentioned above, the analysis of collective creep in terms of individually moving vortices applies only for a limited regime at $B = B_{sv}$. However, with increasing applied field the relative importance of the interaction between the vortices grows and for larger field values, $B_{sv} \leq B$ we enter to the collective or elastic creep, where thermal fluctuations become large due to large flux creep [122-130]. It was now strongly experimentally established that, the line B_{sp} can be well explained by a plastic creep model based on dislocation mediated motion of vortices similar to diffusion of dislocations in atomic solids [122-130]. The activation energy U_{pl} for the motion of a dislocation in the vortex lattice can be estimated as

$$U_{pl} = \frac{1}{4\pi\gamma} e_0 a_0 \propto B^{-1/2}. \quad (111)$$

One notices that U_{pl} decreases with field in contrast to the collective creep activation energies U_{el} , which increases with field. The fishtail peak location B_{sp} can be determined from the condition $U_{pl} = U_{el}$. Using the logarithmic solution of the flux diffusion equation we find

$$U_{el} = kT \ln \frac{t}{t_0}. \quad (112)$$

Balance between the U_{pl} and U_{el} energies gives an expression for the temperature dependence of B_{sp} . To roughly estimate the crossover field and equate the values of the elastic and plastic pinning barriers [122], the following relation can be used

$$\frac{e_0}{\gamma\sqrt{B_{sp}}} = kT \ln t. \quad (113)$$

From the last relation we find

$$B_{sp} = \Phi_0^2 \frac{e^2 e_0^2}{(kT)^2} \propto e_0^2. \quad (114)$$

Inserting the values of the penetration depth λ to the equation for the B_{sp} we obtain the temperature dependence of the transition field, as it is demonstrated in Fig. 13. Note, that a similar temperature dependence $B_{sp}(T)$ was found in some experiments [116] for the melting line. This interesting similarity may support previous claims [117] that the plastic motion of defects in the vortex lattice is a precursor to the melting transition.

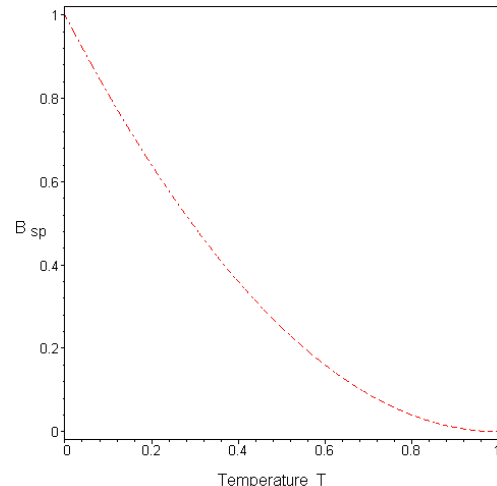


Fig.13. Second magnetization peak field as a function of temperature.

In Fig. 13 we show the temperature dependence of the peak field. Thus, our analysis of the vortex-dynamics shows that the onset of the second magnetization peak occurring at B_{on} is formed by a crossover in the pinning mechanism, from single to collective pinning as the field increases. On the other hand, the temperature dependence of the second magnetization peak B_{sp} can be well explained by the last expression for the plastic vortex creep model.

§5. 3. Order disorder transition

The nature of the different vortex phases in the mixed state of high temperature superconductors is a topic of extensive experimental and theoretical research [49, 143-146]. Much of the experimental work has been focused on the highly anisotropic (BSCCO) crystals, revealing a rich phase diagram [143, 145, 146]. In particular, recent local magnetization measurements [143] in BSCCO crystals revealed a sharp onset of an anomalous second magnetization peak at a field B_{on} , which was interpreted as indicating a transition between two solid phases of the vortex structure. An evidence for two distinct solid vortex phases in BSCCO was previously obtained in neutron diffraction [145] and mSR [146] experiments. Following these observations, a theoretical model was developed [147-149], describing a mechanism for a disorder-induced transition, from a relatively ordered vortex lattice, to a highly disordered vortex state.

An experimental studies have shown [153, 154] that the sample exhibits a distinct second peak, i.e., a strong increase in the magnitude of the magnetization in an intermediate field range. The lowest of these is B_{on} denoting the onset field of the second peak while the peak maximum occurs at B_{sp} . At low fields the elastic interactions govern the structure of the vortex solid, forming a quasicrystalline lattice [150]. Above the onset field B_{on} , disorder dominates and vortex interactions with pinning centers result in an entangled solid where cells of the vortex lattice are twisted and dislocations proliferate [147-149]. To understand the origin of the onset peak it is very useful to study the temperature dependence of the field B_{on} . By considering the competition between the elastic energy of the vortex system and the pinning energy [147-149] it has been suggested that the second peak can result from a transition of a low-field quasicrystalline vortex phase to a disordered vortex solid at higher fields, induced by the quenched disorder. According to recent theoretical model [147-149], the vortex phase diagram is determined by the interplay between three energy scales: the vortex elastic energy E_{el} , the energy of thermal fluctuations E_{th} and the pinning energy E_p . The competition between the first two determines the melting line while the competition between the last two determines the irreversibility line. The competition between the elastic energy and the pinning energy determines the order-disorder transition field B_{on} . We now study the temperature dependence of the onset field, within the framework of a theoretical model [147-149], based on the phenomenological Lindemann criterion for the regime of single vortex pinning [52]. The order-disorder occurs when the disorder-induced wandering of the flux lines is comparable to the lattice constant a_0 and the vortex system loses its translational order and transforms into an disordered phase, in which vortices better adapt to the local pinning potential.

To describe the order-disorder phase transition line, we use the following Lindemann criterion

$$\langle u^2(L_0, 0) \rangle = c_L^2 a_0^2, \quad (115)$$

where $\langle u \rangle$ describes the mean relative displacement of neighboring flux lines caused by the disorder. This Lindemann criterion leads to the usual condition for the order-disorder transition at low temperatures, when the thermal fluctuation is negligible. The Lindemann number c_L is introduced here as a phenomenological parameter that is supposed to depend only weakly on the specific lattice parameters of the solid phase, in particular it is assumed to be independent of the magnetic field. Strictly speaking, the value of the constant c_L may depend on whether the order-disorder transition occurs in the single vortex pinning region or in the region of bundle pinning. However, to understand the essence of the matter, we shall use the simplest approximation: c_L will be considered as the same constant for the various regimes of pinning. We, therefore, use this value in our calculations.

The physics of a single vortex line in point disorder exhibits two different scaling regimes depending on the typical size of the disorder-induced mean-square displacement

$$\langle [u(L) - u(0)]^2 \rangle = u_c^2 \left[\frac{L}{L_c} \right]^{2\zeta}, \quad (116)$$

of a vortex segment of length L , where $\langle \dots \rangle$ denotes the full statistical average to be taken over dynamical variables first and then over the quenched variables describing the disorder, ζ is so-called static critical exponent. We have to carefully distinguish several pinning regimes depending on the size of the pinning length L_c in comparison to the single-vortex length L_0 . For short vortex lengths $L_0 < L_c$ displacements are small

$$\langle u^2(L_c) \rangle \simeq \xi^2,$$

perturbation theory is valid, and we can work with Larkin's random forces [141]. Fluctuations around the ground state of the line are Gaussian in this random force regime and we find a roughness exponent $z = 3/2$, i.e.,

$$\langle [u(L) - u(0)]^2 \rangle = \xi^2 \left[\frac{L}{L_c} \right]^3.$$

This regime is valid up to the collective pinning or Larkin length L_c which is defined by the condition

$$\langle u^2(L_c) \rangle = \xi^2.$$

Longer segments explore many almost degenerate minima of the pinning energy landscape such that fluctuations are non-Gaussian. In this so-called random manifold regime the roughness exponent is known exactly $z = 5/2$ [155]. The currently most reliable estimate for general n is $z = 5/8$ for the vortex line in the bulk superconductor. Therefore we find

$$\langle [u(L) - u(0)]^2 \rangle = u_c^2 \left[\frac{L}{L_c} \right]^{5/4}.$$

On scales exceeding the Larkin length $L_c < L_0$, the vortices start to explore many minima of the disorder potential [155]. This regime is referred to as the random manifold regime [155, 151]. In the case $L_c < L_0$ the pinning energy becomes

$$E_p = U_{dp} \left[\frac{L_0}{L_c} \right]^{1/5}, \quad (117)$$

where

$$U_{dp} = \left(\frac{\delta e_0 \xi^4}{\gamma^4} \right)^{1/3}.$$

By comparing the pinning E_p and elastic energies E_{el} we now derive the transition field

$$B_{on} = B_0 \left[\frac{T_0}{U_{dp}} \right]^3, \quad (118)$$

$$B_0 = \frac{c\Phi_0}{\xi^2}, \quad T_0 = \frac{c e e_0 \xi}{2}.$$

Each vortex remains individually pinned in the presence of thermal fluctuations until the thermal energy T is greater than the typical depinning energy U_{dp} of each single vortex. After further analytical calculation we obtain the following formula to describe the temperature dependence of the transition field

$$B_0 = \frac{c^5 e e_0^2 \Phi_0}{\sqrt{2} \gamma \xi^3}. \quad (119)$$

As we have mentioned above, depending on the type of pinning the crossover field can be either an ascending or descending function of temperature. Substituting the temperature dependencies of the quantities $\xi(T)$, $\lambda(T)$ into the relation (119) and considering the functional form of the disorder parameter, we arrive at the following expressions for δT_c -pinning

$$B_{on} \propto (1 - t^4)^{3/2}. \quad (120)$$

and for δl -pinning

$$B_{on} \propto (1 - t^4)^{-1/2}. \quad (121)$$

respectively.

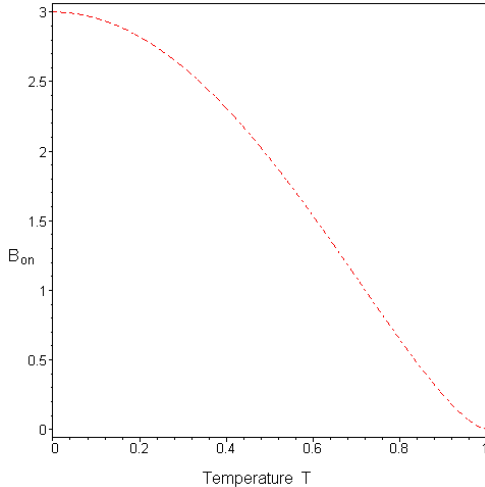


Fig.14. Onset field as a function of temperature.

In Fig. 14 we show the temperature dependence of the onset field. The data in Figure 14 clearly shows that $B_{on}(T)$ for δT_c pinning is a decreasing functions of temperature and therefore this formula can explain the onset of the second magnetization peak, properly.

It is notice able, that onset field B_{on} is inversely proportional to both the anisotropy γ and the disorder parameter γ . Thus, both the anisotropy and disorder may sufficiently affect to the shape of temperature dependencies of both the onset and second magnetization peak field. As has been pointed out Yeshurun et al. [130] that the point disorder induced by electron irradiation can modify the penetration depth λ , anisotropy γ and critical temperature T_c , and thus cause a significant shift of the transition line. Thus, the line $B_{on}(T)$ can be expected to shift lower fields with the introduction of additional disorder in the crystal structure. Calculations [147-149] of B_{on} , based on a Lindemann criterion, confirm this expectation. Other experimental studies Khaikovich et al. [143] of the effect of electron irradiation on the order-disorder transition line have found a systematic decrease of $B_{on}(T)$ with increasing irradiation dose. The decrease in B_{on} is consistent with the enhanced vortex pinning after electron irradiation. Therefore, the quasiordered phase is stabilized by introduction of the point disorder and the strong pinning region is expanded to the lower fields. These results of electron irradiation effect provide further evidence of the field-driven disordering transition scenario [147-149] as a possible origin of $B_{on}(T)$. Specifically, the decrease in the superfluid density n_s with increasing doping at high temperatures increases the magnetic penetration length λ , hence decreases $B_{on} \propto \lambda^{-4}$. It can be concluded that introduction of even a small amount of disorder into very clean systems changes the phase diagram drastically by lowering the order-disorder transition line $B_{on}(T)$ and also changing it's temperature dependence. When the disorder reaches a certain threshold, however, introducing additional disorder does not continue this tendency. With other words, in highly disordered systems, the vortex matter phase diagram is relatively robust with respect to variations in the exact degree of disorder [156-158].

Conclusion

In the present paper we studied the flux jump instabilities of the critical state in conventional and high- T_c superconductors. We have determined the flux jump field and critical state stability criterion within framework of Bean's model. To determine flux jumps threshold an analytical simulations of coupled equations for the magnetic, electric field inductions and temperature has been performed. The field of the first flux jumps is calculated analytically using the dynamic and the adiabatic approximations. The qualitative analysis of the magnetic flux jumps instabilities for superconductors is provided.

Acknowledgements

This study was supported by the Volkswagen Foundation Grant.

References

1. P. S. Swartz and S. P. Bean, *J. Appl. Phys.*, 39, 4991, 1968.
2. C. P. Bean, *Rev. Mod. Phys.*, 36, 31, 1964.
3. H. London, *Phys. Lett.*, 6, 162, 1963.
4. S. L. Wipf, *Phys. Rev.*, 161, 404, 1967; L. S. Wipf, *Cryogenics* 31, 936 1992.
5. H. R. Hart, *J. Appl. Phys.*, 40, 2085, 1969.
6. R. Hansox, *Phys. Lett.*, 16, 208, 1965.
7. M. G. Kremlev, *Cryogenics*, 14, 132, 1974.
8. R. G. Mints and A. L. Rakhmanov, *Instabilities in superconductors*, Moscow, Nauka, 362, 1984.
9. R. G. Mints and A. L. Rakhmanov, *Rev. Mod. Phys.*, 53, 551, 1981.
10. R. G. Mints, *Phys. Rev.*, B 53, 12311, 1996.
11. R. G. Mints and E.H. Brandt, *Phys. Rev.*, B 54, 12421, 1996.
12. M. M. Mola, S. Hill, J. S. Qualls and J. S. Brooks, *Int. J. Mod. Phys.*, B 15, 3353, 2001.
13. H. A. Radovan and R. J. Zieve, *Phys. Rev. B* 68, 224509, 2003.
14. E. R. Novak, O. W. Taylor, Li Liu, H. M. Jaeger, and T. I. Selinder, *Phys. Rev.*, B 55, 11702, 1997.
15. S. Khene and B. Barbara, *Solid State Comm.*, 109, 727, 1999.
16. M. N. Wilson, *Superconducting Magnet*, Oxford University Press, London, 131, 1986.
17. A. Nabialek, M. Niewdzas, H. Dabkowski, J. P. Castellán, and B. D. Gaulin, *Phys. Rev.*, B67, 024518, 2003.
18. M. E. McHenry, H. S. Lessure, M. P. Maley, J. Y. Coulter, I. Tanaka, and H. Kojima, *Physica C* 190, 403, 1992.
19. M. Guillot, M. Potel, P. Gougeon, H. Noel, J. C. Levet, G. Couteau, and J.S. Tholence, *Phys. Lett.*, A 127, 363, 1988.
20. J. Vanacken, L. Trappeniers, K. Rosseel, I. N. Goncharov, V.V. Moshchalkov, Y. Bruynseraede, *Physica C* 332, 411, 2000.
21. G. Fuchs, C. Wenger, A. Gladun, S. Gruss, P. Schaetzle, G. Krabbes, J. Fink, K.H. Muller and L. Schultz, *EUCAS-99 Conference*.
22. Z. W. Zhao, S. L. Li, Y. M. Ni, H. P. Yang, Z. Y. Liu, H. H. Wen, *Phys. Rev. B* 65, 064512, 2002.
23. K. H. Muller and C. Andrikidis, *Phys. Rev. B* 49, 1294, 1994.
24. V. V. Chabanenko, A. I. D'yachenko, A. V. Chabanenko, M. V. Zalutsky, H. Szymczak, S. Piechota and A. Nabialek, *Superconduct. Sci. Technol.*, 1, 1181, 1998.
25. S. Vasilev, V. V. Chabanenko, A. Nabialek, V. Rusakov, S. Piechota and H. Szymczak, *Acta Physica Polonica A*, 106, 777, 2004; S. Vasilev, A. Nabialek, V. Chabanenko, V. Rusakov, S. Piechota, H. Szymczak, *Acta Phys. Pol. A* 109, 661, 2006; A. Nabialek, S. Vasilev, V. Chabanenko, V. Rusakov, S. Piechota, H. Szymczak, *Acta Phys. Pol. A*, 114, 2008; S. Vasilev, A. Nabialek, V.F. Rusakov, L.V. Belevtsov, V. V. Chabanenko and H. Szymczak, *Acta Phys. Pol. A*, 118, 2010; V. Rusakov, S. Vasilev, V. V. Chabanenko, A. Yurov, A. Nabialek, S. Piechota and H. Szymczak, *Acta Phys. Pol. A*, 109, 2006.
26. V. V. Chabanenko, V. F. Rusakov, V. A. Yampol'skii, S. Piechota, A. Nabialek, S.V. Vasilev, and H. Szymczak, *cond-mat. 0106379*, 2002.
27. J. I. Gittleman and B. Rosenblum, *Journ. Appl. Phys.*, 39, 2617, 1968.
28. R. G. Mints and A.L. Rakhmanov, *J. Phys.*, D 12, 1929, 1979.
29. G. Kumm, U. Ring and K. Winzer, *Cryogenics*, 36, 255, 1996.
30. S. Shimamoto, *Cryogenics*, 14, 568, 1974.
31. I. L. Maksimov and R. G. Mints, *J.Phys.*, D 13, 1689, 1980.
32. N. H. Zebouni, A. Venkataram, G. N. Rao, C. G. Grenier, and J. M. Reynolds, *Phys. Rev. Lett.*, 13, 606, 1964.
33. P. G. de Gennes and J. Martison, *Rev. Mod. Phys.*, 36, 45, 1964.
34. A. C. Bodi, I. Kirschner, R. Laiho, and E. Lahderanta, *Solid State Comm.*, 98, 1049, 1996.
35. I. Legrand, I. Rosenmann, Ch. Simon, G. Collin, *Physica C* 211, 239, 1993.
36. L. Legrand, I. Rosenman, R. G. Mints, G. Collin and E. Janod, *Europhys. Lett.*, 34, 287, 1996.
37. A. Gurevich, *Appl. Phys. Lett.*, 78, 1891, 2001.
38. G. L. Dorofeev, A.B. Imenitov, and E. Yu. Klimenko, *Cryogenics* 20, 307, 1980.
39. R. G. Mints and A. L. Rakhmanov, *J. Phys.*, D 15, 2297, 1982.
40. D. Monier and L. Fruchter, *Eur. Phys. J.*, B 3, 143, 1998.
41. A. M. Campbell and J. E. Evetts, *Critical current in superconductors*, London, 1972.
42. A. Gurevich and H. Kupfer, *Phys. Rev.*, B 48, 6477, 1993.
43. A. P. Malozemoff, *Physica C*, 185, 264, 1999.
44. Z. J. Huang, Y. Y. Xue, H. H. Feng, and C. W. Chu, *Physica C*, 184, 371, 1991.
45. D. Shi and M. Xu, *Phys. Rev.*, B 44, 4548, 1991.
46. Y. Yeshurun and A. P. Malozemoff, *Phys. Rev. Lett.*, 60, 2202, 1988.
47. H. G. Schnack, R. Griessen, J. G. Lensink, C. J. van der Beek, and P. H. Kes, *Physica C* 197, 337, 1992.
48. A. Gurevich and E. H. Brandt, *Phys. Rev. Lett.*, 73, 178, 1994.
49. G. Blatter, M. V. Feigel'man, V. B. Geshkenbein, A. I. Larkin, V. M. Vinokur, *Rev. Mod. Phys.*, 66, 1125, 1994.
50. M. P. Fisher, *Phys. Rev. Lett.*, 62, 1415, 1989.
51. Y. Yeshurun, A. P. Malozemoff, and A. Shaulov, *Rev. Mod. Phys.*, 68, 911, 1996.
52. V. Feigel'man, V. B.Geshkenbein, and V. M. Vinokur, *Phys. Rev. Lett.*, 63, 2303, 1989.

53. P. H. Kes, J. Aarto, J. van den Berg, C. J. van der Beek, and J. A. Mydosh, *Supercon. Sci. Technol.*, 1, 242, 1989.
54. J. R. Tompson, Y. R. Sun, and F. Holtzberg, *Phys. Rev. B* 44, 458, 1991.
55. P. W. Anderson, *Phys. Rev. Lett.*, 9, 309, 1962.
56. P. W. Anderson and Y. B. Kim, *Rev. Mod. Phys.*, 36, 39, 1964.
57. C. S. Pande and R. A. Masumura, *Physica C* 332, 292, 2000.
58. L. Burlachkov, D. Giller, and R. Prozorov, *condmat-9802076*, 1998.
59. E. Zeldov, N. M. Amer, G. Koren, A. Gupta, M. W. McElfresh and R. J. Gambino, *Appl. Phys. Lett.*, 56, 680, 1990.
60. E. H. Brandt, *Phys. Rev. B* 55, 14513, 1997.
61. Y. Mawatari, A. Sawa, H. Obara, M. Umeda, and H. Yamasaki, *Appl. Phys. Lett.*, 70, 2300, 1997.
62. A. Gerber, J. N. Li, Z. Tarnawski, J. J. M. Franse, and A. A. Menovsky, *Phys. Rev.*, B 47, 6047, 1993.
63. Z. Wang and D. Shi, *Solid State Commun.*, 90, 405, 1994.
64. T. Nattermann, *Phys. Rev. Lett.*, 64, 2454, 1990.
65. N. A. Taylanov, *cond-mat.*, 0207009, 2002.
66. R. P. Huebener, *Super. Sci. Technol.*, 8, 189, 1995.
67. T. Sasaki, K. Watanabe, and N. Kobayashi, *Sci. Rep.*, RITU A 42, 351, 1996.
68. A. T. Fiory and B. Serin, *Phys. Rev. Lett.*, 16, 308, 1966.
69. A. T. Dorsey, *Phys. Rev. B* 46, 8376, 1992.
70. P. Ao, *J. Low. Temp. Phys.*, 107, 347, 1997.
71. R. P. Huebener, and A. Seher, *Phys. Rev.*, 181, 701, 1969.
72. S. N. Artemenko, and A. F. Volkov, *JETP*, 70, 1051, 1976.
73. A. V. Gurevich and R. G. Mints, *JETP Lett.*, 31, 52, 1980.
74. A. N. Larkin and Yu. N. Ovchinnikov, *JETP*, 49, 2337, 1981.
75. V. L. Ginzburg and G. F. Jarkov, *Uspekh. Fiz. Nauk*, 125, 19, 1978.
76. N. B. Kopnin, *Zh. Eksp. Teor. Fiz.*, 69, 364, 1975.
77. R. Solomon and F. A. Otter, *Phys. Rev.*, 164, 608, 1967.
78. C. Caroli, P. G. DeGennes, and J. Matrison, *Phys. Lett.*, 9, 307, 1964.
79. L. D. Landau and E. M. Lifshitz, *Statistical Physics*, Moscow, Nauka, 1976.
80. C. A. Duran, P. L. Gammel, R. E. Miller, D. J. Bishop, *Phys. Rev.*, B 52, 75, 1995.
81. V. Vlasko-Vlasov, U. Welp, V. Metlushko, and G. W. Crabtree, *Physica C*, 341-348, 1281, 2000.
82. T. H. Johansen, M. Basiljevich, D. V. Shantsev, P. E. Goa, Y. M. Galperin, W. N. Kang, H. J. Kim, E. M. Choi, M. S. Kim, S. I. Lee, *Europhys. Lett.*, 59, 599, 2002.
83. A. V. Bobyl, D. V. Shantsev, Y. M. Galperin, A. A. F. Olsen, T. H. Johansen, W. N. Kang and S. I. Lee, *cond-mat. 0304603*, 2003.
84. F. L. Barkov, D. V. Shantsev, T. H. Johansen, W. N. Kang, H. J. Kim, E. M. Choi, and S. I. Lee, *Phys. Rev.*, B 67, 064513, 2003.
85. P. Leiderer, J. Boneberg, P. Brull, V. Bujok, S. Herminghaus, *Phys. Rev. Lett.*, 71, 2646, 1993.
86. U. Bolz, D. Schmidt, B. Biehler, B. U. Runge, R. G. Mints, K. Numssen, H. Kinder, P. Leiderer, *Physica C* 388, 715, 2003.
87. U. Bolz et al., *Europhys. Lett.*, 64, 517, 2003.
88. M. S. Welling et al., *Physica C* 411, 11, 2004.
89. I. A. Rudnev et al., *Cryogenics*, 43, 663, 2003.
90. A. L. Rakhmanov, D. V. Shantsev, Y. M. Galperin and T. H. Johansen, *cond-mat/0405446*, 2004.
91. I. Aronson, A. Gurevich, and V. V. Vinokur, *Phys. Rev. Lett.*, 87, 067003, 2001.
92. I. S. Aranson et al., *Phys. Rev. Lett.* 94, 037002, 2005.
93. D. V. Denisov, A. L. Rakhmanov, D. V. Shantsev, Y. M. Galperin, T. H. Johansen, *Phys. Rev. B* 73, 014512, 2006.
94. M. R. Wertheimer and J. G. Gilchrist, *J. Phys. Chem. Solids* 28, 2509, 1967.
95. G. T. Seidler, C. S. Carrillo, T. F. Rosenbaum, U. Welp, G. W. Crabtree, and V. M. Vinokur, *Phys. Rev. Lett.*, 70, 2814, 1993.
96. P. Bak, C. Tang and K. Wiesenfeld, *Phys. Rev. Lett.*, 59, 381, 1987.
97. P. Bak, C. Tang and K. Wiesenfeld, *Phys. Rev.*, A 38, 3645, 1988.
98. R. J. Zieve, T. F. Rosenbaum, H. M. Jaeger, G. T. Seidler, G. W. Crabtree, and U. Welp, *Phys. Rev.*, B 53, 11849, 1996.
99. C. J. Olson, C. Reichhardt and F. Nori, *Phys. Rev.*, B 56, 6175, 1998.
100. K. E. Bassler and M. Paczuski, *Phys. Rev. Lett.*, 81, 3761, 1998.
101. S. Field, J. Witt and F. Nori, *Phys. Rev. Lett.*, 74, 1206, 1995.
102. O. Pla and F. Nori, *Phys. Rev. Lett.*, 67, 919, 1991.
103. R. A. Richardson, O. Pla and F. Nori, *Phys. Rev. Lett.*, 72, 1268, 1994.
104. R. Cruz, R. Mulet and E. Altshuler, *Physica A* 275, 15, 2000.
105. G. Mohler and D. Stroud, *Phys. Rev.*, B 60, 9738, 1999.
106. R. Mulet and E. Altshuler, *Physica C* 281, 317, 1997.
107. C. M. Aegerter, M. S. Welling, and R. J. Wijngaarden, *cond-mat. 0305591*, 2003.
108. W. Barford, *Phys. Rev.*, B 56, 425, 2002.
109. E. Altshuler and T. H. Johansen, *cond-mat. 0402097*, 2004.
110. K. Behina, C. Capan, D. Mailly, and B. Etienne, *Phys. Rev.*, B 61, 3815, 2000.
111. S. Majumdar, M. R. Lees, G. Balakrishnan, and D. McK Paul, *cond-mat. 0305208*, 2003.
112. A. Milner, *Physica B* 294, 388, 2001.

113. A. Gerber, A. Milner, *Phys. Rev.*, B 62, 9753, 2000.
114. A. Terentiev, D. B. Watkins, L. E. De Long, L. D. Cooley, D. J. Morgan, and J. B. Ketterson, *Phys. Rev.*, B 61, R9249, 2000.
115. S. B. Roy and P. Chaddah, *Physica C* 279, 1, 1997.
116. H. Safar, P. L. Gammel, D. A. Huse, D. J. Bishop, W. C. Lee, and D. M. Ginsberg, *Phys. Rev. Lett.* 70, 3800, 1993.
117. W. K. Kwok, J. A. Fendrich, C. J. van der Beek, and G. W. Crabtree, *Phys. Rev. Lett.* 73, 2614, 1994.
118. P. L. Gammel, U. Yaron, Y. P. Ramirez, D.J. Bishop, A. M. Chang, R. Ruel, L. N. Pfeiffer, E. Bucher, G. D'Anna, D. A. Huse, K. Mortensen, M. R. Eskildsen, and P. H. Kes, *Phys. Rev. Lett.* 80, 833, 1998.
119. M. Daemling, J. M. Seutjens, and D. C. Laralestier, *Nature (London)* 346, 332, 1990.
120. L. Klein, E. R. Yacoby, Y. Yeshurun, A. Erb, G. Muller-Vogt, V. Breit, and H. Wuhl, *Phys. Rev. B* 49, 4403, 1994.
121. L. Krusin-Elbaum, L. Civale, V. M. Vinokur, and F. Holtzberg, *Phys. Rev. Lett.* 69, 2280, 1992.
122. Y. Abulafia, A. Shaulov, Y. Wolfus, R. Prozorov, L. Burlachkov, Y. Yeshurun, D. Majer, E. Zeldov, H. Wuhl, V.B. Geskenbein, and V. M. Vinokur, *Phys. Rev. Lett.* 77, 1596, 1996.
123. D. Giller, A. Shaulov, Y. Yeshurun, and J. Giapintzakis, *Phys. Rev. B* 60, 106, 1999.
124. D. Giller, A. Shaulov, R. Prozorov, Y. Abulafia, Y. Wolfus, L. Burlachkov, Y. Yeshurun, E. Zeldov, and V. M. Vinokur, J. L. Peng, and R. L. Greene, *Phys. Rev. Lett.* 79, 2542, 1997.
125. Y. V. Bugoslavsky, A. L. Ivanov, A. A. Minakov, and S.I. Vasyurin, *Physica C* 233, 67, 1994.
126. V. Hardy, A. Wahl, A. Ruyter, A. Maignan, C. Martin, L. Coudrier, J. Provost, and C. Simon, *Physica C* 232, 347, 1994.
127. A. Maignan, S.N. Putilin, V. Hardy, C. Simon, and B. Raveau, *Physica C* 266, 173, 1996.
128. T. Aouaroun and C. Simon, *Physica C* 306, 238, 1998.
129. M. Pissas, D. Stampoulos, E. Moraitakis, G. Kallias, D. Niarchos, and M. Charalambous, *Phys. Rev. B* 59, 121, 1999.
130. V. Yeshurun, N. Bontemps, L. Burlachkov and A. Kapitulnik, *Phys. Rev. B* 49, 1548, 1994.
131. R. Yoshizaki, I. Ikeda and J. D. Jeon, *Physica C* 225, 299, 1994.
132. G. Yang, P. Shang, S. D. Sutton, I. P. Jones, J. S. Abell, and C. E. Gough, *Phys. Rev. B* 48, 4054, 1993.
133. F. Zuo, S. Khizroev, G. C. Alexandrakakis, and V. N. Kopylov, *Phys. Rev. B* 52, R755, 1995.
134. N. Chikumoto, M. Konczykowski, N. Motohira, and A. P. Malozemoff, *Phys. Rev. Lett.* 69, 1260, 1992.
135. Y. Kopelevich, and P. Esquinazi, *J. Low Temp. Phys.*, 113, 1998.
136. P. Esquinazi, A. Setzer, D. Fuchs, Y. Kopelevich, E. Zeldov and C. Assmann, *Phys. Rev.*, B 60, 17, 12454, 1999.
137. A. Yu. Galkin, Y. Kopelevich, P. Esquinazi, A. Setzer, V.M. Pan, and S. N. Barilo, *cond-mat.* 9912346, 1999.
138. A. Pan, M. Ziese, R. Hohne, P. Esquinazi, S. Knappe, and H. Koch, *Physica C* 301,72 1998; A. Pan, R. Hohne, M. Ziese, P. Esquinazi, and C. Assmann, in *Physics and Material Sciences of Vortex States, Flux Pinning and Dynamics*, edited by R. Kossowsky et al.(Kluwer Academic), Dordrecht, 545, 1999.
139. Y. Kopelevich, S. Moehlecke, J. H. Torres, R. Ricardo da Silva, and P. Esquinazi, *J. Low. Temp. Phys.*, 116, 261, 1999.
140. D. Stamopoulos, A. Speliotis, and D. Niarchos, *Supercond. Sci. Technol.*, 17, 1261, 2004.
141. A. I. Larkin and Yu. N. Ovchinnikov, *J. Low Temp. Phys.* 34, 409, 1979.
142. A. A. Zhukov, H. Kupfer, G. Perkins, L. F. Cohen, A. D. Caplin, S. A. Klestov, H. Claus, V. I. Voronkova, T. Wolf and H. Wuhl, *Phys. Rev.*, B 51, 12704, 1995.
143. B. Khaykovich, E. Zeldov, D. Majer, T. W. Li, P. H. Kes, and M. Konczykowski, *Phys. Rev. Lett.* 76, 2555 1996; E. Zeldov, A. Larkin, V. Geshkenbein, M. Konczykowski, D. Majer, B. Kheykovich, V. Vinokur, and H. Shtrikham, *Phys. Rev. Lett.* 73, 1428, 1994.
144. A. Schilling, R. A. Fisher, N. E. Phillips, U. Welp, D. Dasgupta, W. K. Kwok, and G. W. Crabtree, *Nature* 382, 791 1996.
145. R. Cubitt, E. M. Forgan, G. Yang, S. L. Lee, D. M. Paul, H. A. Mook, M. Yethiraj, P. H. Kes, T. W. Li, A. A. Menovsky, Z. Tarnawski, and K. Mortensen, *Nature (London)* 365, 407 1993.
146. S. L. Lee et al., *Phys. Rev. Lett.* 71, 3862, 1993.
147. D. Ertas and D. R. Nelson, *Physica (Amsterdam)* 272C, 79, 1996.
148. V. Vinokur, B. Khaykovich, E. Zeldov, M. Konczykowski, R.A. Doyle, and P. Kes, *Physica C* 295, 209, 1998.
149. T. Giamarchi and P. Le Doussal, *Phys. Rev. B* 55, 6577, 1997.
150. T. Giamarchi and P. Le Doussal, *Phys. Rev. Lett.* 72, 1530, 1994.
151. J. Kierfeld, T. Nattermann, and T. Hwa, *Phys. Rev. B* 55, 626, 1997.
152. D. S. Fisher, *Phys. Rev. Lett.* 78, 1964, 1997.
153. S. Kokkalis, P. A. J. de Groot, S. N. Gordeev, A. A. Zhukov, R. Gagnon, and L. Taillefer, *Phys. Rev. Lett.* 82, 5116, 1999.
154. Y. Paltiel, E. Zeldov, Y. Myasoedov, M. L. Rappaport, G. Jung, S. Bhattacharya, M. J. Higgins, Z. L. Xiao, E. Y. Andrei, P. L. Gammel, and D.J. Bishop, *Phys. Rev. Lett.* 85, 3712, 2000.
155. T. Halpin-Healy, Y. C. Zhang, *Phys. Rep.* 254, 215, 1995.
156. T. Nishizaki, T. Naito, and N. Kobayashi, *Phys. Rev. B* 58, 11169, 1998.
157. T. Nishizaki, T. Naito, S. Okayasu, A. Iwase, and N. Kobayashi, *Phys. Rev. B* 61, 3649, 2000.
158. J. Karpinski, S. Kazakov, M. Angst, A. Mironov, M. Mali, and J. Roos, *Phys. Rev. B* 64, 094518, 2001.